

Secondary Compression of Clay Soils

Ali Hossien Basheer Garoushi

Submitted to the
Institute of Graduate Studies and Research
in partial fulfillment of the requirement for the degree of

Master of Science
in
Civil Engineering

Eastern Mediterranean University
September 2017
Gazimağusa, North Cyprus

Approval of the Institute of Graduate Studies and Research

Assoc. Prof. Dr. Ali Hakan Ulusoy
Acting Director

I certify that this thesis satisfies the requirements as a thesis for the degree of Master of Science in Civil Engineering.

Assoc. Prof. Dr. Serhan Şensoy
Chair, Department of Civil Engineering

We certify that we have read this thesis and that in our opinion it is fully adequate in scope and quality as a thesis for the degree of Master of Science in Civil Engineering.

Asst. Prof. Dr. Eriş Uygur
Supervisor

Examining Committee

1. Prof. Dr. Zalihe Sezai

2. Assoc. Prof. Dr. Huriye Bilsel

3. Asst. Prof. Dr. Eriş Uygur

ABSTRACT

In this thesis, the behavior of secondary compression of a selected clay soil from Famagusta is assessed by conducting series of one-dimensional consolidation tests on samples prepared with various initial void ratios and water contents. The testing program consists of standard oedometer tests (SOT) and long term creep tests (CT) where the samples are subjected to preconsolidation stress prior to application of a sustained effective stress for a period of seven days.

The analysis of the test results indicated that, the coefficient of secondary compression for soft samples increases up to an effective stress of 50 kPa and then gradually decreases and becomes approximately constant with increasing effective stress. The coefficient of secondary compression for compacted samples is observed to increase with increasing vertical effective stress up to an effective stress of approximately 2.5 times preconsolidation stress, staying approximately constant with respect to further increase in effective stress. For overconsolidated samples, the coefficient of secondary compression increased with reduction in the degree of overconsolidation. The rate of secondary compression decreased with log time for all samples. The maximum value of the coefficient of secondary compression occurred in the Log time range of 100 min to 1000 min for all samples. A creep function, previously proposed by (Yin, 1999) is applied on the measured creep curves, the function indicated a good fit to the measured creep curves for all samples.

Keywords: Creep, Soft clay, Secondary compression, Standard oedometer test.

ÖZ

Gazimağusa’da mevcut bir şişen kil’in ikincil oturma davranışı odömetre deneyleri ile, değişik su muhtevası ve boşluk oranında hazırlanan deney numuneleri ile çalışılmıştır. Deney programı, standart odömetre deneyleri ve uzun vadeli oturma deneyleri (creep) içermektedir, bu deneylerde değişik efektif gerilmelerde ön yüklemeli olarak hazırlanmış numunelere yedi güne kadar varan sürelerde sabit yük uygulanmıştır.

Deney sonuçlarının analizi göstermiştir ki, yumuşak numuneler için ölçülen ikincil oturma katsayısı 50kPa efektif gerilmeye kadar artmakta ve daha sonraki efektif gerilme artışlarına göre azalarak yaklaşık sabit bir değere ulaşmaktadır. Sıkıştırma uygulanmış numunelerde ikincil oturma katsayısı, efektif gerilme artarken, ön gerilme değerinin yaklaşık iki buçuk katına kadar artmış, daha fazla efektif gerilme artışı olduğunda ise yaklaşık olarak sabit kalmıştır. Ön gerilme uygulanmış numunelerde ikincil oturma katsayısı, aşırı konsolidasyon olma derecesi düştükçe artmıştır. Bütün numuneler için ikincil oturma zamanın logaritmasına göre azalmıştır. Bütün numuneler için en yüksek ikincil oturma 100dak ile 1000dak logaritma zaman aralığında elde edilmiştir. Daha önce Yin (1999) tarafından önerilmiş bir ikincil oturma fonksiyonu ölçümler üzerinde denenmiş ve bunların tümü ile iyi derecede bir uyum içerisinde olduğu gözlemlenmiştir.

Anahtar kelimeler: İkincil oturma, Yumuşak kil, Standart odömetre deneyi.

ACKNOWLEDGMENT

I would like to thank Asst. Prof. Dr. Eriş Uygur for his continuous support and guidance in the preparation of this study. Without his invaluable supervision, all my efforts could have been short-sighted.

I owe quite a lot to my family who allowed me to travel all the way from Libya to Cyprus and supported me all throughout my studies. I would like to dedicate this study to them as an indication of their significance in this study as well as in my life.

My unlimited appreciation is toward the academic and non-academic staff of civil engineering department, Eastern Mediterranean University, North Cyprus for their patience, assistance, advice and encouragement. Also, my warm regards to any lecturer who enlarged my academic knowledge. I also feel compelled to thank my colleagues in North Cyprus and in Libya for encouraging me during my studies.

TABLE OF CONTENTS

ABSTRACT.....	iii
ÖZ.....	iv
ACKNOWLEDGMENT.....	v
LIST OF TABLES.....	ix
LIST OF FIGURES.....	x
LIST OF SYMBOLS AND ABBREVIATIONS.....	xii
1 INTRODUCTION.....	1
1.1 Background.....	1
1.2 Research Objectives.....	2
1.3 Aim of the Study.....	3
1.4 Research Limitation.....	3
1.5 Scope of Work.....	3
2 LITERATURE REVIEW.....	5
2.1 Introduction.....	5
2.2 Compressibility Behavior of Clay Soils.....	5
2.2.1 One-dimensional Compression Curve.....	5
2.2.2 Compressibility Curve.....	7
2.2.3 Secondary Compression.....	10
2.3 Coefficient of Secondary Compression ($C\alpha$) and Vertical Effective Stress.....	14
2.4 Variation of the Coefficient of Secondary Compression with Time.....	18
2.5 Summarized Critical Review.....	22
3 METHODOLOGY AND EXPERIMENTAL STUDY.....	24
3.1 Introduction.....	24

3.2 Sampling Location and Local Geology.....	24
3.2.1 The Superficial Deposits of Famagusta.....	24
3.2.2 Soil Sampling	25
3.3 Testing Strategy	26
3.4 Preparation of the Soft Samples.....	27
3.5 Preparation of the Compacted Samples	29
3.5.1 Soil Compaction.....	29
3.5.2 Sample Preparation for Testing.....	29
3.6 Testing Methods.....	32
3.6.1 Standard Oedometer Test, SOT.....	32
3.6.2 Creep test.....	32
3.7 Results of Index and Classification Tests	33
3.7.1. Initial Moisture Content	33
3.7.2 Particle Size Distribution.....	33
3.7.3 Specific Gravity.....	33
3.7.4 Plasticity Index	34
3.7.5 Soil Classification.....	35
4 RESULTS, ANALYSIS AND DISCUSSION	36
4.1 Introduction.....	36
4.2 Analysis of Compressibility Behavior Using Standard Oedometer Tests	37
4.2.1 Compression Curves at Each Test Stage.....	37
4.2.2 Comparison of Compressibility Curves	39
4.2.3 Analysis of Secondary Compression Behavior using Standard Oedometer Tests.....	41
4.3 Analysis of Secondary Compression Behavior Using Creep Tests	46

4.3.1 Assessment of Vertical Strain Curves for Soft Samples	46
4.3.2 Analysis of Secondary Compression of Compacted Samples.....	54
4.4 Summarized Critical Review	57
5 CONCLUSION	59
REFERENCES.....	64
APPENDICES	69
Appendix A : Test Reports for Standard Oedometer Tests.....	70
Appendix B : Test Reports for Creep Tests.....	75

LIST OF TABLES

Table 2.1: Values of compression index for several types of soil.....	7
Table 2.2: Soil classification in according to C_{α}	13
Table 2.3: Values of C_{α}/C_c for various types of soils.....	14
Table 4.1: Coefficient of secondary compression for soft and compacted samples for standard oedometer tests.....	44
Table 4.2: Non linear fitting curve parameters for sot samples.....	52
Table 4.3: Coefficient of secondary compression for soft samples.....	53
Table 4.4: Coefficient of secondary compression for compacted samples.....	55
Table 4.5: Non linear fitting curve parameters for compacted samples.....	55

LIST OF FIGURES

Figure 2.1: Standard oedometer curve	6
Figure 2.2: Typical compression lines	8
Figure 2.3: Computing of preconsolidation pressure.....	9
Figure 2.4: Determination of the coefficient of secondary compression.....	12
Figure 2.5: The bi-linear relationship between $C\alpha$ and Cs^*	13
Figure 2.6: Types of compression curves	21
Figure 2.7: Comparison between measured curve and fitted curve.....	22
Figure 3.1: Site location	25
Figure 3.2: Soil sampling	26
Figure 3.3: Testing strategy and testing groups for soft sample (GR-1).....	28
Figure 3.4: Testing strategy and testing groups of samples compacted using standard Proctor energy (GR-2).....	29
Figure 3.5: Testing strategy and testing groups of samples compacted with increased energy (GR-3)	29
Figure 3.6: Stages of sample preparation for soft samples	31
Figure 3.7: Compaction curves for GR-2 and GR-3	32
Figure 3.8: Particle size distribution test result.....	34
Figure 3.9: Liquid limit test results for natural state method.....	35
Figure 3.10: Liquid limit test results for drying pulverizing method.....	36
Figure 4.1: Compressibility curves from standard oedometer test, GR-1.....	38
Figure 4.2: Compressibility curves from standard oedometer test, GR-2.....	39
Figure 4.3: Compressibility curves from standard oedometer test, GR-3.....	39

Figure 4.4: Standard oedometer compressibility curves for soft and compacted samples.....	41
Figure 4.5: Creep curves from standard oedometer test for, GR-1	42
Figure 4.6: Creep curves from standard oedometer test for, GR-2.....	43
Figure 4.7: Creep curves from standard oedometer test for, GR-3.....	43
Figure 4.8: Variation of $C\alpha$ with t_p (min).....	45
Figure 4.9: Variation of $C\alpha$ with vertical effective stress in standard oedometer tests	46
Figure 4.10: Vertical strain curves of GR-1.1 ($P_c=50$ kPa)	47
Figure 4.11: Vertical strain curves of GR-1.2 ($P_c=100$ kPa)	47
Figure 4.12: Vertical strain curves of GR-1.3 ($P_c=200$ kPa)	48
Figure 4.13: Vertical strain curves of GR-1.4 ($P_c=300$ kPa)	48
Figure 4.14: The relationship observed between preconsolidation stress and vertical strain upon unloading, obtained after 24 hours.....	49
Figure 4.15: Vertical strain creep curves of GR-1.1	50
Figure 4.16: Vertical strain creep curves of GR-1.2	51
Figure 4.17: Vertical strain creep curves of GR-1.3	51
Figure 4.18: Vertical strain creep curves of GR-1.4	52
Figure 4.19: Creep curves of compacted samples subjected to standard Energy GR-2	57
Figure 4.20: Creep curves of compacted samples subjected to increased energy GR-3	57

LIST OF SYMBOLS AND ABBREVIATIONS

C_c	Compression index
C_r	Recompression Index
σ'_v	Vertical effective stress
C_v	Coefficient of consolidation
C_α	Coefficient of secondary compression for time interval 100 min to 1000 min
C_{α^*}	Coefficient of secondary compression for time interval 1000 min to 10000 min
e	Void ratio
Δe	Change in void ratio
a_v	Coefficient of compressibility
ρ_w	Density of water
t_p	Time corresponding to the end of primary consolidation.
m_v	Compressibility coefficient
P_c	Preconsolidation stress
G_s	Specific gravity
$+\epsilon_v$	Vertical strain of swell
$-\epsilon_v$	Vertical strain of compression
$\Delta\epsilon$	Creep strain
$\Delta\epsilon_1$	Creep strain limit
ψ_0	Initial creep strain
t	Creep time at strain of $\Delta\epsilon$
t_0	Initial creep time.

a_s	Zero consolidation
ΔH	Change in height per log cycle of time
H_i	Initial height of the specimen
C_s^*	Swell index
n	Number of drops per layer.
N	Number of layers.
w	Weight of hammer
h	Free fall height
v	Volume of the mold
m	Secondary compression factor.
w_c	Water Content
ASTM	American Society for Testing and materials
CH	High Plasticity Clay
CT	Creep Test
GR-1	Soft Sample
GR-2	Compacted Sample with Standard Energy
GR-3	Compacted Sample with Increased Energy
LL	Liquid Limit
OCR	Over Consolidation Ratio
PL	Plastic Limits
SOT	Standard Oedometer Test
NaCl	Salt Water
OWC	Optimum Water Content

Chapter 1

INTRODUCTION

1.1 Background

Clay soils are complicated natural materials, that contain particle size diameter less than 0.002 mm. Clay soils are considered significant in construction works due their complex physical, which have a critical influence on the compressibility characteristics. Clay soils are very important in geotechnical engineering because of their complex behavior:

- High plasticity clays (generally plastic Index $>30\%$, or $LL > 50\%$) pose high swelling and shrinkage potential with change in moisture content and may cause excessive total and differential deformations to structures.
- Clays generally have low hydraulic conductivity. The higher the plasticity, the lower is hydraulic conductivity.
- In natural state, clay soils generally have moisture content and their deformation under loads is generally consists of two parts: immediate deformation and time-dependent deformation (consolidation and creep)- consolidation is due to dissipation of excess pore-water pressures and creep is due to plastic deformation of soil structure.
- Pore-water pressure play a major role in strength and deformation of clayey soils under various loading conditions.
- Chemistry of pore water can significantly affect the behavior of the clay soil.

- Strength and deformation properties of the clayey soils depends on their loading history.

In general, consolidation of clay soils is a process of compression corresponding to excess pore water pressure due to an effect of vertical stress. The compressibility of the clay soils is measured in the laboratory using oedometer test by performing various load increments. However, the compressibility can be divided as follows:

- 1- Initial compression, where the compression occurs due to compression of air in the voids.
- 2- Primary compression, where the consolidation occurs due to excess of pore water pressure.
- 3- Secondary compression, which occurs under constant effective stress after dissipation of the pore water pressure due to rearrangement of soil particles.

However, secondary compression, usually referred as creep, can be expressed by the coefficient of secondary compression C_{α} , which is a critical element of prediction of long term settlement for designing roads and foundations.

1.2 Research Objectives

The overall aim of this thesis is to investigate the creep behavior of a selected superficial deposit from Famagusta. The specific objectives are as follows:

- To investigate the creep behavior using two methods of sample preparation and evaluate the creep from each method.
- Discuss the compressibility parameters under various test conditions such as initial void ratio, initial water content, and preconsolidation stress.

- To examine the variation of the coefficient of secondary compression with time in logarithmic scale.
- Give some recommendations about calculation of the coefficient of secondary compression.
- To study the impact of vertical effective stress on the secondary compression during normally consolidated and overconsolidated conditions.

1.3 Aim of the Study

The fundamental purpose of this thesis is to study the creep characteristics of a clay soil using laboratory tests and analysis of test results for preconsolidation stress and two methods of sample preparation; uncompacted and compacted.

1.4 Research Limitation

Although the aims of the research are attained, there are still unavoidable limitations that can be summarized

follows:

- Due to time limitation, only one soil type is examined using two methods of sample preparation.
- Only one-dimensional consolidation test is used to measure the compressibility.
- Hence, the study only focuses on the vertical strain by assuming there isn't any horizontal strain during creep.

1.5 Scope of Work

The main goal of this thesis is to gain an understanding of the mechanism of creep. This is accomplished by a survey of previous studies then designing laboratory program, after analyzing the test results a conclusion is made. The thesis contains five chapters as follows:

In the second chapter, a literature review about compressibility behavior of clay soils involving the overview of the theory of one-dimensional consolidation, secondary compression, and non-linear creep are presented.

The laboratory program including soil sampling, testing strategy, methods of sample preparation, index properties, soil classification and testing methods are presented in the third chapter.

The fourth chapter is dedicated for computing compressibility parameters and analysis of the oedometer test results. As a first part, the compressibility of standard oedometer test and the creep results are presented and analyzed. A significant part of chapter four involves creep tests, where the coefficient of secondary compression is deeply studied.

In the last chapter, chapter five, conclusion and recommendations are summarized by providing general comments from chapter three and four.

Chapter 2

LITERATURE REVIEW

2.1 Introduction

In this chapter, a brief review about compressibility behavior of clay soils and the theory of secondary compression are presented. The compressibility behavior of soft clays and compacted clays are generally reviewed and summarized. The variation of long term compression with time and the influence of vertical effective stress are reviewed. The geotechnical parameters defining compressibility behavior that used in this thesis are identified.

2.2 Compressibility Behavior of Clay Soils

2.2.1 One-dimensional Compression Curve

The interpretation of graphical plot of the one-dimensional compression corresponding to time in logarithmic scale in a standard oedometer test is proposed by Casagrande (Head, 1986). A one-dimensional compressibility curve obtained in a standard oedometer tests is shown in Figure 2.1 which consists of three parts; initial convex parabolic curve, then a linear part and then a final part which the time is closer to concave parabolic form. The time corresponding to zero consolidation can be found by choosing two points on the first part of the curve (A and B), where the difference in time between them is 1:4, the vertical distance between them is

calculated and added to the vertical data of the first point, which is interpreted to correspond to zero consolidation a_s .

The point at which 100% consolidation is achieved during the test can be obtained by extending the linear part of the initial compression and intersecting this with the extend of the linear part of the final compression curve; the projection of this point on the vertical axis a_{100} corresponds to 100% consolidation. The part of the curve beyond this point is known as secondary compression curve, which occurs under constant effective stress after the dissipation of the excess pore water pressure is completed.

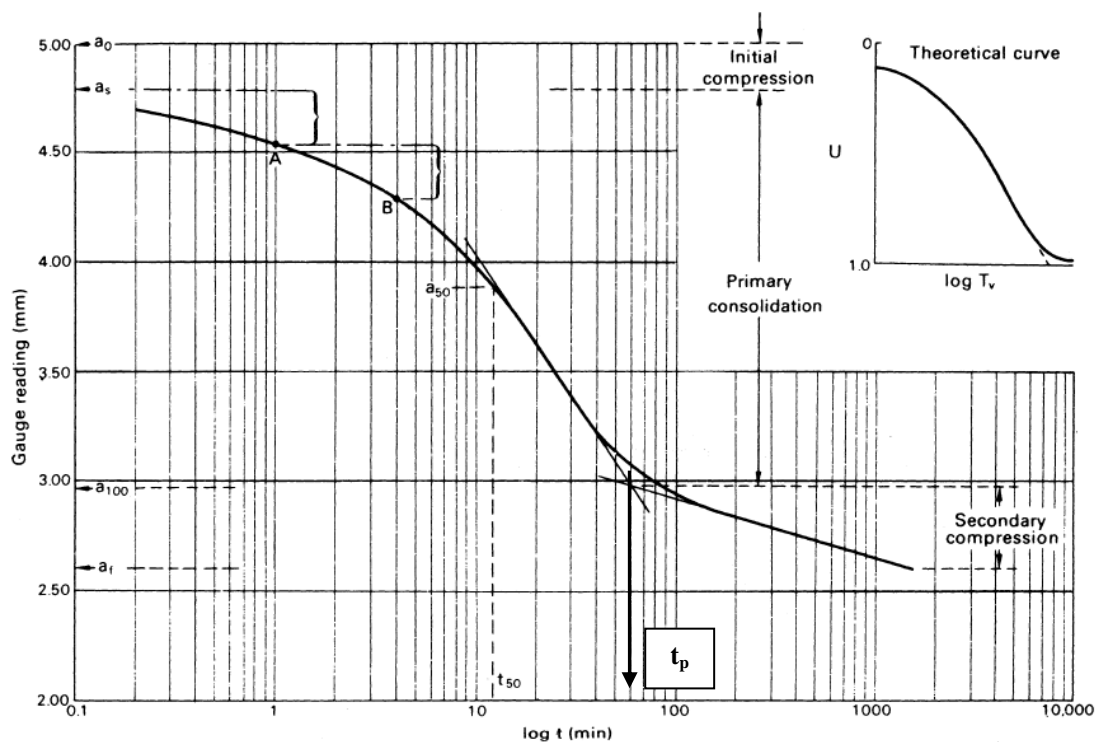


Figure 2.1: Standard oedometer curve (Craig, 2004)

t_p : The time corresponding to the end of primary consolidation as shown in Figure 2.1.

2.2.2 Compressibility Curve

In Figure 2.2 typical plot of void ratio against vertical effective stress in semi-logarithmic paper. The first stage of the curve is called overconsolidated condition where the soil has experienced pre-stress more than the applied effective stress. The second part of the curve is linear where the soil is in normal consolidated condition, the linear part is known as virgin compression line in which the vertical effective stress is higher than any pre-stress the soil has ever experienced. The slope of the virgin compression line is primary compression index C_c , the recompression line is linked with the virgin line and the slope of the recompression curve is the recompression index C_r , (Craig, 2004). Typical values of compression index for several types of soils are illustrated in Table 2.1.

Table 2.1: Values of compression index for several types of soil (Jain et al., 2015).

Type of soil	Compression index C_c
Dense sand	0.0005- 0.01
Loose sand	0.025- 0.05
Firm clay	0.03- 0.06
Stiff clay	0.06- 0.15
Medium soft clay	0.15- 1.0
Organic soil	1.0-4.5

The preconsolidation stress can be defined as the maximum stress that the soil has ever experienced in the past. The method of calculating preconsolidation stress of a soil is proposed by Casagrande (Craig, 2004) as shown in Figure 2.3. The back straight line BC is extended and the point which has the maximum curvature D is

obtained, after extending the line AD and producing horizontal line from point D, the angle between the two lines is divided with a bisector, the intersection point g on the horizontal axis is the preconsolidation stress.

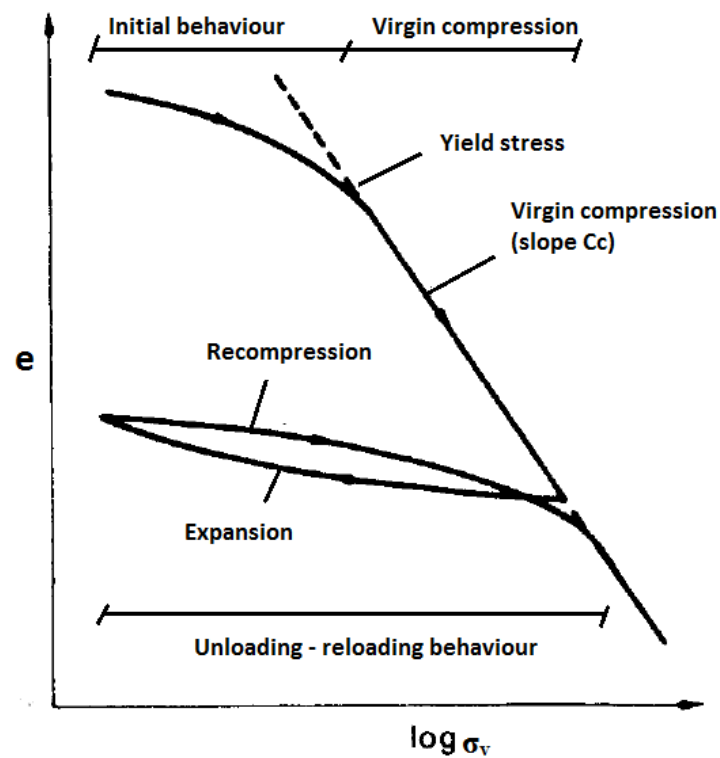


Figure 2.2: Typical compression lines (Craig, 2004)

Compressibility parameters can be obtained from standard oedometer. In a standard oedometer test, the parameters for obtaining magnitude of compression behavior are considered to be; compression index C_c , recompression index C_r , coefficient of volume compressibility m_v , and the coefficient of secondary compression C_α , as described by (Head, 1986).

$$C_c = \frac{-\Delta e}{\Delta (\log_{10} \sigma'_v)} \quad (2.1)$$

where,

C_c : compression index.

Δe : change in void ratio during virgin compression line.

$\Delta (\log_{10} \sigma'_v)$: change in vertical effective stress in logarithmic scale.

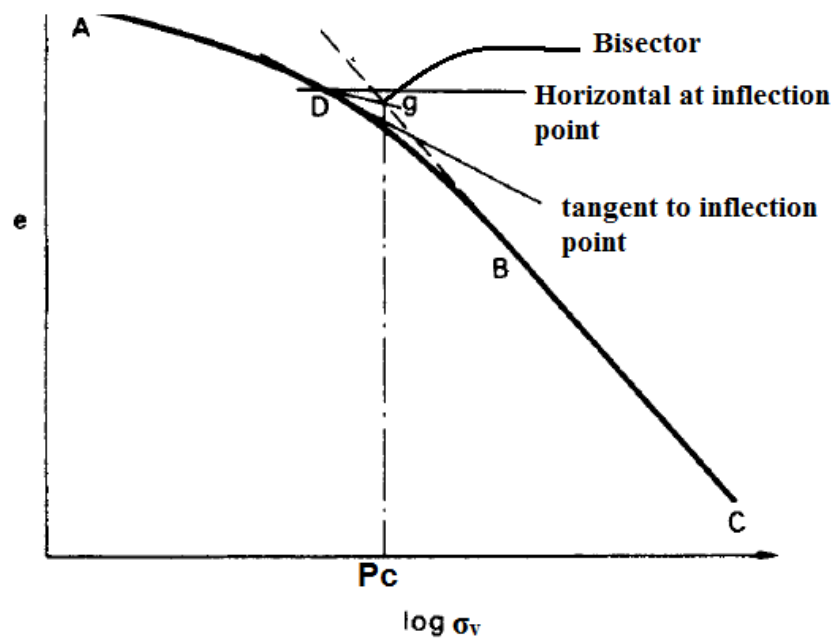


Figure 2.3: Computing of preconsolidation pressure (Craig, 2004)

P_c : the preconsolidation stress.

$$C_r = \frac{-\Delta e}{\Delta (\log_{10} \sigma'_v)} \quad (2.2)$$

where,

C_r : primary swell index.

Δe : change in void ratio during recompression line.

$\Delta (\log_{10} \sigma'_v)$: change in vertical effective stress in logarithmic scale.

The recompression index is usually referred to compression index, the correlation between C_r and C_c within the range 0.02 to 0.2 for almost all soils, (Terzaghi et al., 1996).

$$m_v = \frac{a_v}{1+e} \quad (2.3)$$

where,

m_v : coefficient of volume compressibility.

a_v : coefficient of compressibility.

e : void ratio.

The time- dependency is obtained simply by calculation of the coefficient of consolidation C_v using Terzaghi's one- dimensional consolidation theory (Head, 1986).

$$C_v = \frac{a_v}{m_v * \rho_w} \quad (2.4)$$

where,

C_v : coefficient of consolidation.

ρ_w : density of water.

2.2.3 Secondary Compression

After Terzaghi proposed his outstanding theory of one dimensional consolidation of soils in 1923 based on excess pore water pressure dissipation, laboratory results and field observations have shown that the settlement continues even after the dissipation completes (Fatahi et al., 2012). In order to distinguish the two components of the compression, the term of 'primary consolidation' is used to describe the time dependent process due to the change in volume induced by the expulsion of water from the voids, and transferring load from the pore water pressure to the soil particles. On the other hand, creep or so-called secondary compression is generally

defined as the deformation under a constant effective stress. It is necessary to exclude creep phenomenon from the deformation under constant load because the effective stresses can be variable under a constant load. The research on the long-term settlement of soils has become important and been developed for many decades (Fatahi et al., 2012).

The coefficient of secondary compression $C\alpha$ is usually used to describe the secondary compression which can be obtained from Casagrande method (Head, 1986), as:

$$C\alpha = \frac{\Delta H}{H_i} \text{ per one log cycle of time.} \quad (2.5)$$

where,

$C\alpha$: coefficient of secondary compression.

ΔH : change in height per log cycle of time.

H_i : initial height of the specimen.

$C\alpha^*$: coefficient of secondary compression computed from time interval between 1000 min to 10000 min.

The main objective of calculating $C\alpha^*$ is to examine the variation of the coefficient of secondary compression with time.

The above formulation assumes that the variation of secondary compression is linear in log time space. Figure 2.4 shows the determination of coefficient of secondary compression Head (1986).

Deng et al. (2012) investigated the correlation between the coefficient of secondary compression and swell index, the test results showed that the relationship is bi-linear in which there are two slopes, the first slope is related to rebounding and the second slope is related to swelling as shown in Figure 2.5.

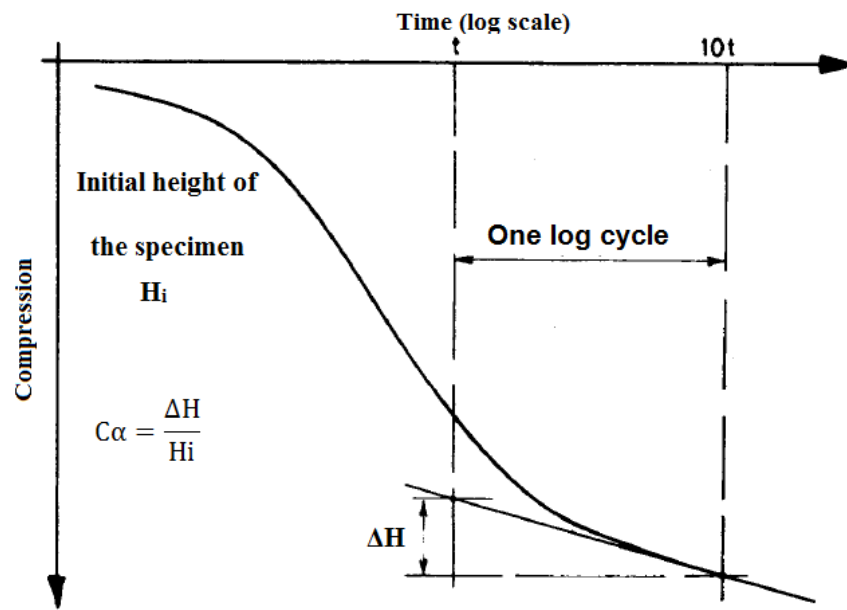


Figure 2.4: Determination of the coefficient of secondary compression (Head, 1986)

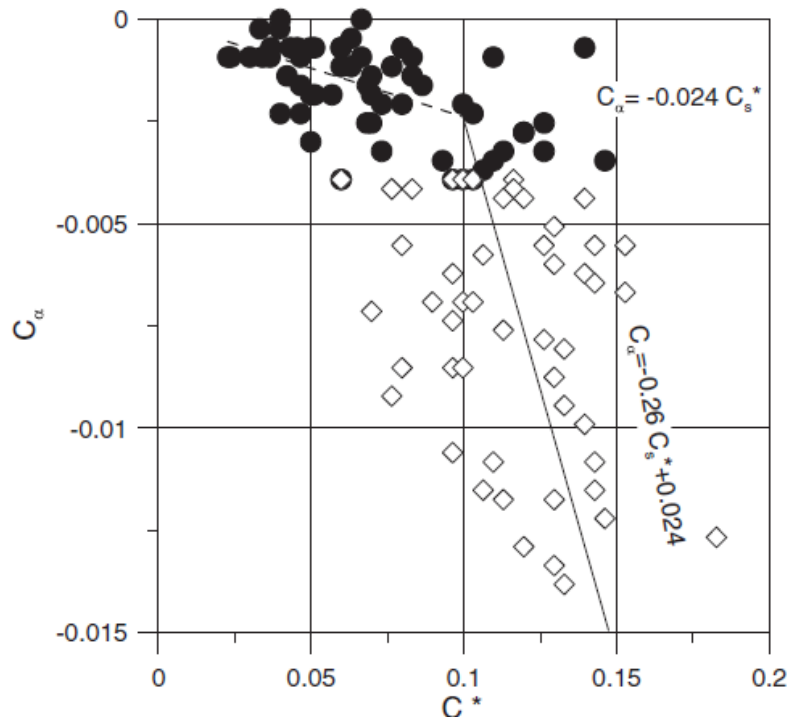


Figure 2.5: The bi-linear relationship between $C\alpha$ and Cs^* (Deng et al., 2012)

where, Cs^* is the swell index.

Mesri et al. (1973) studied the significance of secondary compression and noted that coefficient of secondary compression is an effective parameter to evaluate secondary compression. Mesri et al. (1973) also stated that physicochemical condition and mineral structure of soil have huge impact on secondary compression. In addition, they investigated the influence of several parameters on secondary compression such as vertical effective stress, pre-stress, remolding, thickness of sample, temperature, and shear stress; they reported that the duration of stress and preconsolidation stress are the most influential parameters that affect secondary compression. Furthermore, they classified secondary compression behavior of soil as presented in Table 2.2.

Mesri and Castro (1987) stated that the correlation between the coefficient of secondary compression $C\alpha$ and compression index Cc is constant for any kind of soil, in which the compression index increased or decreased or remained constant with vertical effective stress at which the coefficient of secondary compression increased or decreased or remained constant with time. In Table 2.3 the values of $C\alpha/Cc$ for inorganic and highly organic clays of soil are presented, (Terzaghi et al., 1996).

Table 2.2: Soil classification in according to $C\alpha$ (Mesri et al., 1973).

$C\alpha$ % (per log cycle)	Secondary compression
-----------------------------	-----------------------

< 0.2	Very low
0.4	Low
0.8	Medium
1.6	High
3.2	Very high
>6.4	Extremely high

Table 2.3: Values of $C\alpha/Cc$ for various types of soil (Terzaghi et al., 1996).

Type of soil	$C\alpha/Cc$
Granular soils	0.02 ± 0.01
Shale and mudstones	0.03 ± 0.01
Inorganic silts, clays	0.04 ± 0.01
Highly organic clays	0.05 ± 0.01
Fibrous peats	0.06 ± 0.01

2.3 Coefficient of Secondary Compression ($C\alpha$) and Vertical Effective Stress

Sridharan and Rao (1982) conducted series of one dimensional consolidation testes to examine the mechanism of secondary compression. The oedometer testes carried out in which there are variations in void ratio, load increment ratio and organic fluids. It is shown that coefficient of secondary compression reduce with increase in vertical effective stress.

Graham et al. (1983) investigated coefficient of secondary compression for Ottawa clays using series of one dimensional consolidation tests, each load increment applied for 10 days. The primary consolidation observed to be ended before 100 min,

the coefficient of secondary compression calculated for strain at of 100 min and 10000 min. The results showed that coefficient of secondary compression with respect to void ratio at a given stress level appears independent of test conditions.

Head (1986) stated that coefficient of secondary compression of peat and highly organic clays increase with increasing vertical effective stress, but he found it to be independent of vertical effective stress for inorganic clays.

Nash et al. (1992) examined secondary compression characteristics using undisturbed and reconstituted samples. The reconstituted samples prepared by mixing distilled water with salt water 21 g/ NaCl for the target of liquid limit, the tests carried out using fixed ring oedometer cell with a height of 20 mm. The test program consisted of incremental loads IL to examine creep characteristics at stress above yield. The coefficient of secondary compression calculated after 16 hours of applying load increment from e-logt curves. The test results showed that secondary compression behavior was small within overconsolidated stage, after samples is reloaded up to insitu preconsolidation stress 45 kPa secondary compression stress increased, the maximum value of the coefficient of secondary compression occurred around twice yield stress at 100 kPa.

AL-Shamrani (1996) investigated the secondary compression of Sabkha soil; the results showed that secondary compression of Sabkha is critical; it is noted that the coefficient of secondary compression was higher when the soil with in overconsolidated condition than normal consolidated condition. AL-Shamrani (1998) examined secondary compression for Sabkha soil using undisturbed samples; the test results showed that coefficient of secondary compression depends on vertical

effective stress. The results indicated increase with effective stress then remained approximately constant.

Matchala et al. (2008) studied the impact of vertical stresses on the coefficient of secondary compression of Marine clays in South Korea. The test results showed that the coefficient of secondary compression increased with increasing vertical effective stress and reached a peak value when stress level is twice preconsolidation stress.

Miao and Kavazanjian (2007) carried out series of one dimensional consolidation tests on undisturbed samples of Jiangsu soft clays. A total of 50 undisturbed samples were investigated, the specimens dimensions were 61.8 mm in diameter and 20 mm in height. The relationship between coefficient of secondary compression and stress ratios (σ'_v / P_c) indicated that coefficient of secondary compression depends on stress level, it increases rapidly for stress level less than 2.5 then became constant for stress level higher than 2.5.

Lingling and Sonyu (2010) conducted series of one dimensional consolidation tests to investigate secondary compression behavior of Lianyungang clays, the program performed on both undisturbed and reconstituted samples, a thin-wall free piston tube is used to excavate high quality undisturbed samples from depth of 6 m below ground surface. The test results showed that coefficient of secondary compression for both undisturbed and reconstituted samples increases with vertical effective stress until reaches maximum value in the vicinity of yield stress then dramatically decreases with increasing vertical stress, it has pointed out that coefficient of secondary compression can be neglected in pre-yield stage. Also coefficient of

secondary compression of undisturbed samples has higher values than reconstituted samples.

Deng et al. (2012) analyzed results of one dimensional consolidation tests of undisturbed samples the clay extracted by coring at north east of Belgium, the results showed that the relationship between coefficient of secondary compression and stress ratio (σ'_v / P_c) increasing linearly on semi-logarithmic scale.

Li et al. (2012) performed series of one dimensional consolidation tests in order to investigate secondary compression of Shanghai clays. The long-term consolidation program consists of three intact specimens and one reconstituted specimens, the reconstituted specimen prepared by mixing the clays with distilled water equal to 1.4 liquid limits. The secondary compression measured for each load increment within period of seven days. They have found that coefficient of secondary compression is approximately linear when stress level in the vicinity of ($OCR=1$), then reduce with time for consolidation stress ratios more than 1. Coefficient of secondary compression for reconstituted specimen found within range (1/3-1/2) of undisturbed specimen.

Luo and Chen (2014) investigated creep behavior of River Delta Clays. Undisturbed samples were extracted from depth of 6 m and 16 m, the consolidation ring has a diameter of 61.8 mm and height of 20 mm is used. The results showed that the relationship between secondary compression and consolidation stress is conditional, with in overconsolidated condition secondary compression increases with increasing effective stress but in normal consolidated condition decrease with increasing effective stress. These results were found in other studied such as (Walker, 1969).

Mehrab et al. (2011) carried out series of one dimensional consolidation tests on undisturbed samples, the samples were taken from eleven sites in Iran. In order to investigate long term settlements each load applied for 1 to 3 weeks, the coefficient of secondary compression is found to be dependent on the ratio between vertical effective stress to preconsolidation pressure (σ'_v/P_c), the maximum value of $C\alpha$ occur at stress ratio between (2.7 – 4.72).

Huayang et al. (2016) examined secondary compression behavior using three types of soft soils: Lin-Gang clays, Genral fishing clays and Qing-Fang clays. Reconstituted specimens were prepared by drying the clays at room temperature then pulverized after that clays is mixed with distilled water until uniform paste achieved, The reconstituted samples prepared for a targets of 1.9-2.28-2.7 liquid limits. The effect of consolidation stress and initial void ratio on the coefficient of secondary compression is investigated; they have found that the characteristic of $C\alpha$ depends on vertical effective stress and initial void ratio. The coefficient of secondary compression increased in order with initial void ratio up to void ratio corresponding to yield stress then $C\alpha$ decreased. In addition, it was observed that coefficient of secondary compression for reconstituted specimens have higher values than undisturbed specimens.

2.4 Variation of the Coefficient of Secondary Compression with Time

Secondary compression is thought to be the compression that takes place after the end of primary consolidation under constant effective vertical stress on e-log_t plot. Coefficient of secondary compression is the slope of secondary compression on e-log_t per load cycle of time (Head, 1986).

Barden (1968) reported that coefficient of secondary compression is not linear on semi logarithmic scale. This finding is also confirmed by (Leroueil et al., 1985).

Fox et al. (1992) performed long-term one-dimensional consolidation tests on Middleton peat; the test results demonstrated the significant of secondary compression to total compression. Compression- log time curves showed that under constant vertical effective stress the coefficient of secondary compression was not constant but increased with Log time.

Mesri et al. (1997) investigated the variation of the coefficient of secondary compression with time of Middleton peat. The coefficient of secondary compression showed lowest value in the recompression range while the highest value was immediately after preconsolidation stage, and remained constant or slightly decreased within normal consolidation stage.

Sridharan and Prakash (1998) suggested new strategy for distinguishing secondary compression in view of secondary compression factor m , as shows in equation 2.6;

$$m = \frac{\Delta \log e}{\Delta \log t} \quad (2.6)$$

where,

m : secondary compression factor.

e : Void ratio.

t : Time

The benefit of this technique is that the charactering of secondary compression showed as linear compression over long time span. In the cases of $(\log e - \log t)$

secondary compression factor is more reliable tool to calculate coefficient of secondary compression than non-linear secondary compression tail. (e-log t) method proposed by Terzaghi can be used for soil that shows linear secondary compression where C_{α} can be shown as linear line on semi-logarithmic scale.

Mesri and Vardhanabhuti (2006) assessed reliable laboratory results and field observation of wide variety of natural deposits, it is concluded that characteristics of coefficient of secondary compression varies with time, it may increase or remain constant or decrease. The long term monitoring of coefficient of secondary compression found to be decrease with in almost all cases.

Nurly and Yulindasari (2007) conducted series of oedometer testes on peat, undisturbed block sampling from West Johor –Malaysia is investigated. Secondary compression curves derived for two different methods, first method is (e-logt) proposed by Terzaghi (Head, 1986), the other method is secondary compression factor (log e – log t) proposed by (Sridharan and Prakash, 1998). The oedometer test results showed that C_{α} varies with log time when using (e-logt). The method of secondary compression factor (log e – log t) can be reliable for estimating C_{α} since secondary compression shows as straight line. The disconnection point between primary compression and secondary compression is significant for estimation of C_{α} when using secondary compression factor method. Nurly and Yulindasari (2007) stated that there are three types of compression- log time curve as shown in Figure 2.6. In which most of compression- log time curves placed in type 1 which usually referred as (S) curve. In curve 2, the secondary compression curve does not show linear with time and primary consolidation is rapid. In curve 3, the inflection point

between primary and secondary compression is not well defined and t_p can not well predict.

Linchang Miao and Edward Kavazanjian (2007) stated that there are two problems with the relationship between (strain-log time). One problem is that the origin of time is not well defined. However, this problem becomes less and less significant as the end time of primary consolidation increases. A second problem is that when the time is infinite, the semi-logarithmic relationship yields a settlement (or strain) that is infinite. Thus, the semi-logarithmic function may cause a serious error in the estimation of the long-term settlement.

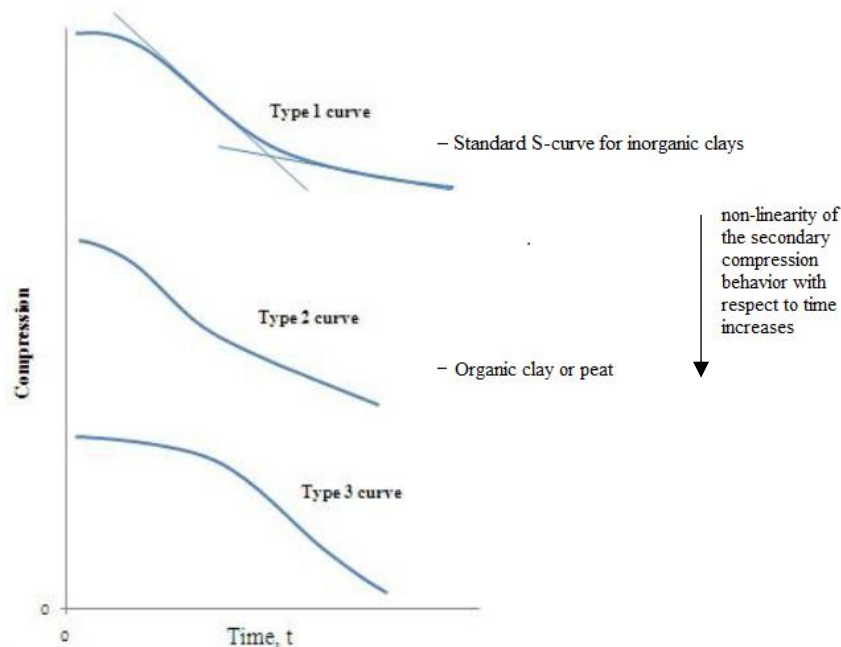


Figure 2.6: Types of compression curves (Nurly and Yulindasari, 2007)

Yin (1999) conducted series of one-dimensional consolidation tests investigating marine deposits for Hong Kong, the soil extracted from a depth about 2 m. The soil

contained of 27.5% clays, 58.4% silts and 14.1% fine sand. The author proposed non-linear creep formula that describes the creep behavior as follows:

$$\Delta\varepsilon = \frac{\psi_0 \ln[(t+t_0)/t_0]}{1+(\psi_0+\Delta\varepsilon_1) \ln[(t+t_0)/t_0]} \quad (2.7)$$

where,

$\Delta\varepsilon$: Creep strain.

$\Delta\varepsilon_1$: Creep strain limit.

ψ_0 : Initial creep strain

t: Creep time at strain of $\Delta\varepsilon$.

t_0 : Initial creep time.

The proposed formula indicated good fitting between measured and computed data as shown in Figure 2.7. (Yin, 1999).

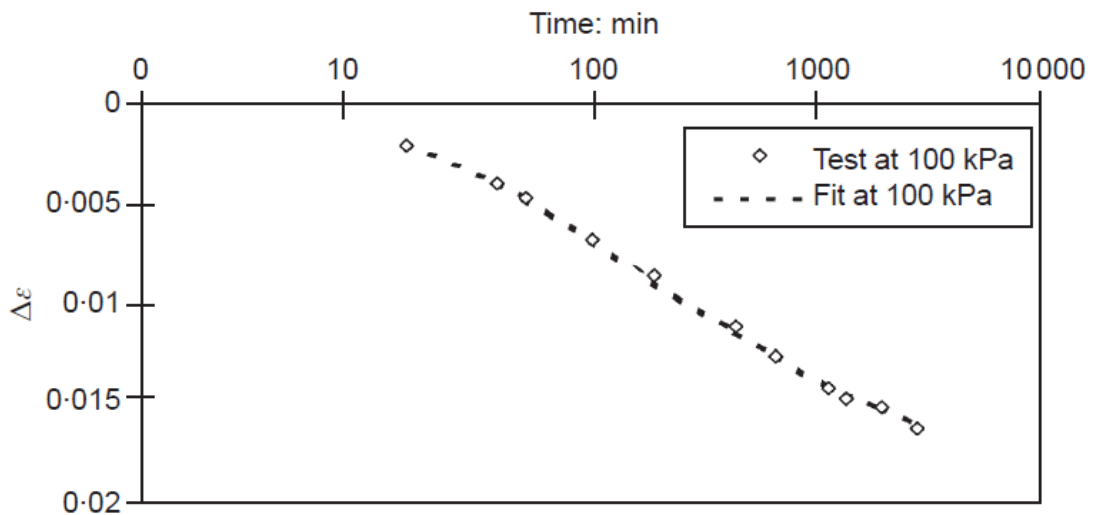


Figure 2.7: Comparison between measured curve and fitted curve (Yin, 1999)

2.5 Summarized Critical Review

The literature review as introduced in section 2.3 and 2.4 the cover the follow:

The coefficient of secondary compression $C\alpha$ is influenced strongly by effective stress and pre-stress.

There is argue about how do secondary compression behavior change with vertical effective stress, in some cases increases or remain constant or decrease. In this study, the effect of consolidation pressure on the secondary compression will be investigated during overconsolidation stage and normal consolidation stage.

In almost all cases, secondary compression was not constant with time on semi logarithmic scale under constant effective stress in some cases found to be increased or remained constant or decreased. The variation of secondary compression with time is studied.

The coefficient of secondary compression $C\alpha$ is powerful parameter to predict secondary compression. There is major problem when calculating coefficient of secondary compression $C\alpha$ from logarithmic scale. The variation of secondary compression is not constant in Log time; it may increases or decreases or remains constant. Thus, calculating $C\alpha$ as slope of $e - \log t$ pre one cycle of time is not accurate because the slope is changing from cycle to another. In fact, coefficient of secondary compression decreases with time under constant stress that in all cases (Mesri and Vardhanabhuti, 2005).

Chapter 3

METHODOLOGY AND EXPERIMENTAL STUDY

3.1 Introduction

In this chapter, the testing strategy and methods followed to investigate the compressibility behavior of soft samples studied and described, all laboratory testing are carried out in accordance with the American standards for testing and materials (ASTM).

3.2 Sampling Location and Local Geology

3.2.1 The Superficial Deposits of Famagusta

The superficial deposits of Cyprus can be divided into five groups, (1) Alluvium, (2) Mesoria clays, (3) Bentonitic clays, (4) Mamonia clays, (5) Degirmenlik clays, as shown in Figure 3.2 (Atalar and Das, 2009). Clay soils of this region are classified as high to extremely high swelling potential, with a liquid limit typically varying in the range from 53 to 91 (Atalar and Das, 2009; Tawfiq and Nalbantoglu, 2009; Malekzadeh and Bilsel, 2012).

3.2.2 Soil Sampling

The soil sample used in this research is taken from the south campus of Eastern Mediterranean University, Famagusta. The approximate location of the sampling site is presented in Figure 3.1. A trial pit of approximately 2 m deep is carried out, a track hoe excavator to enable sampling below the organic soil cover. The approximate coordinates of the sampling location are (35°09'01.4"N, 33°51'29.4"E). Figure 3.2 shows stages of the sampling process.

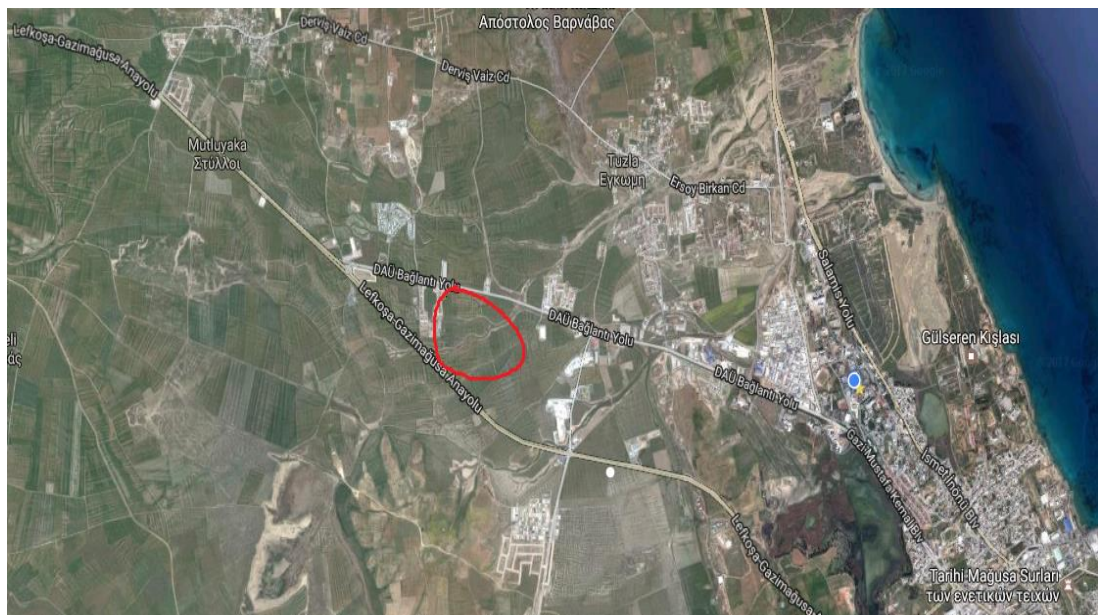


Figure 3.1: Site location (Google maps ©, 2017)



Figure 3.2: Soil sampling

3.3 Testing Strategy

In order to study long term compressibility characteristics (creep) of the soil sample, and at the same time study effects of overconsolidation on the compressibility behavior, a testing strategy is designed. Testing involved three main groups of specimens; (GR-1) soft samples, (GR-2) samples compacted with standard Proctor energy and, (GR-3) samples compacted using increased energy (Section 3.5.2). In this way it is considered that both the effects of soil structure and the degree of overconsolidation on the creep behavior can be studied.

The testing strategy and testing groups are presented in Figure 3.3 to Figure 3.5. The main test groups are subjected to standard oedometer testing in the first stage of testing. Then, identical samples of four sub-groups, four different preconsolidation stages are attained and all are subjected to creep testing, in which consolidation stress is kept constant to match a certain degree of overconsolidation. For soft sample group, these were $OCR = 1$, $OCR = 1.3$, $OCR = 2$ and $OCR = 4$, where OCR is overconsolidation ratio attained prior to creep testing.

Hence,

$$\text{OCR} = \frac{\text{preconsolidation stress attained prior to creep test}}{\text{constant effective stress applied during creep test}} = \frac{P_c}{\sigma'_v} \quad (3-1)$$

3.4 Preparation of the Soft Samples

Soft samples are prepared in according to (Burland, 1990). The soil is used in it is natural state without any drying or pulverizing. Standard compaction mold is used to mix the soil with distilled water using a spatula, targeting liquid limit water content until smooth consistency is obtained. Then the mold is gently tapped from the bottom to minimize air bubbles. After keeping the mold in a vacuum desiccator for 24 hours, 50 mm diameter standard oedometer rings are inserted carefully into the soil slurry and the soft soil samples are extracted and trimmed using a thin wire. Whilst preparing the specimens, the main goal is to prepare them with approximately identical void ratio and water content. Figure 3.6 presents stages of sample preparation for soft samples.

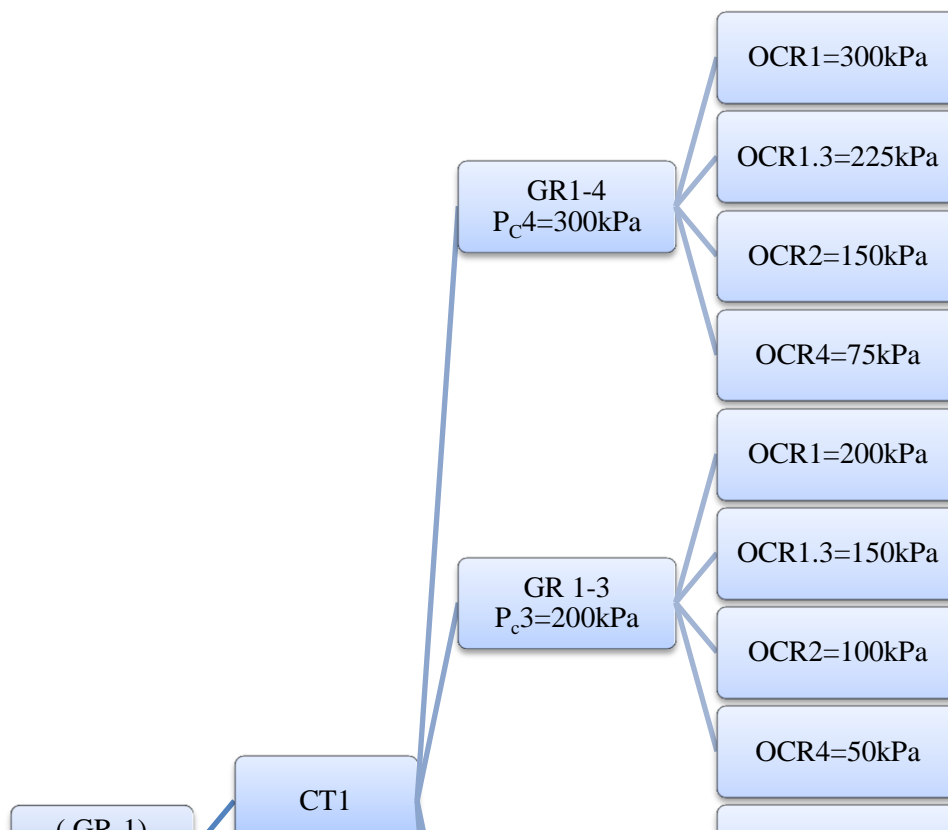


Figure 3.3: Testing strategy and testing groups for soft sample (GR-1)

OCR: Overconsolidation ratio.

CT: Creep test.

P_c : preconsolidation stress.

SOT: Standard oedometer test.

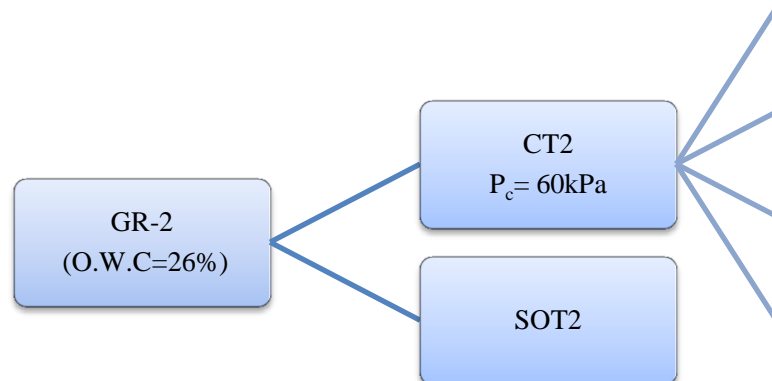


Figure 3.4: Testing strategy and testing groups of samples compacted using standard Proctor energy (GR-2)

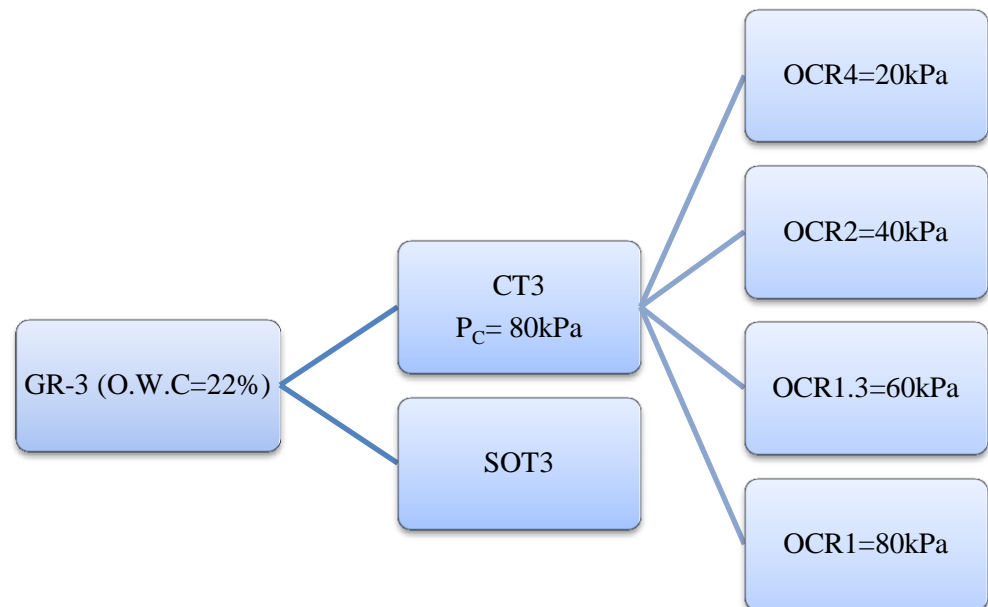


Figure 3.5: Testing strategy and testing groups of samples compacted with increased energy (GR-3)

3.5 Preparation of the Compacted Samples

3.5.1 Soil Compaction

Two different energies are applied in order to obtain different preconsolidation stresses, for two compacted samples. The compaction test carried out included standard Proctor energy on the sample GR-2 and increased energy on the sample GR-3 in which the soil was compacted in five layers and each layer 25 drops. The results of the tests are presented in Figure 3.7. The optimum moisture content for GR-2 and GR-3 are obtained as 26.5 % and 22% respectively.

3.5.2 Sample Preparation for Testing

Energy 1: First, 2 kg of soil is dried in oven at 50°C for five days then pulverized; next the soil is mixed with distilled water at the target of optimum moisture content of 26.5 %. After keeping the soil in vacuum desiccators for 24 hours the soil is compacted using Standard Proctor compaction method.

Energy 2: The method of preparation is similar to Energy 1, except that the compaction is carried out in 5 layers with optimum moisture content = 22%.

In order to calculate energy per unit volume of the soil to compare between energy levels, compaction effort is calculated using the following equation:

$$E = \frac{n \cdot N \cdot w \cdot h}{v} \quad (3.2)$$

were,

n: Number of drops per layer.

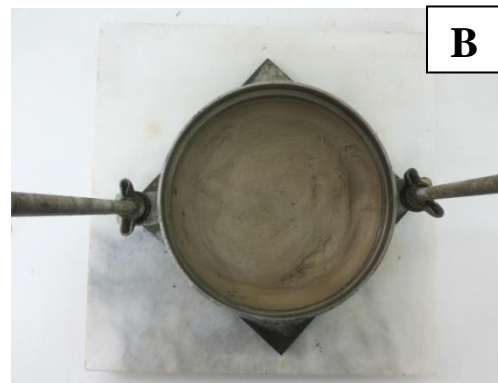
N: Number of layers.

w: weight of hammer

h: free fall height

v: volume of the mold

$$\frac{E_2}{E_1} = \frac{(25 \cdot 5 \cdot 2.5 \cdot 30) / 1000}{(25 \cdot 3 \cdot 2.5 \cdot 30) / 1000} = 1.67 \quad (3.3)$$



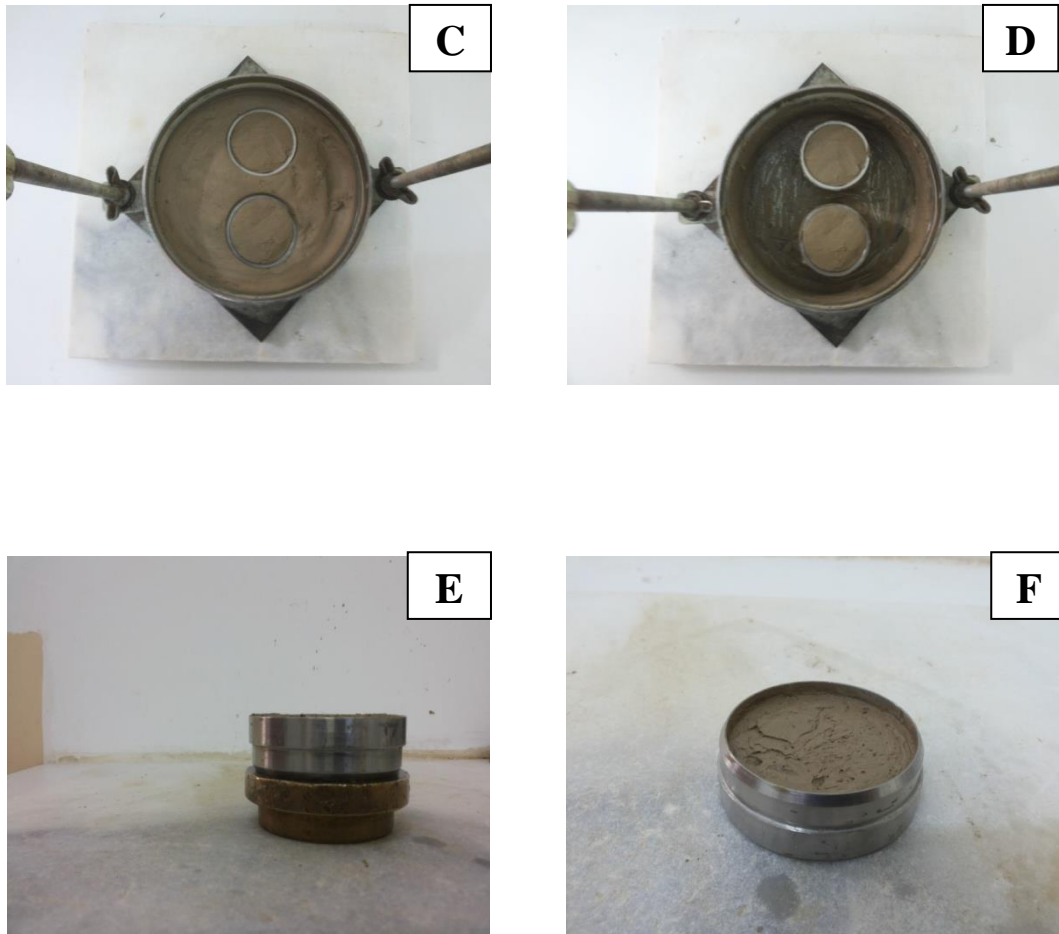


Figure 3.6: Stages of sample preparation for soft samples

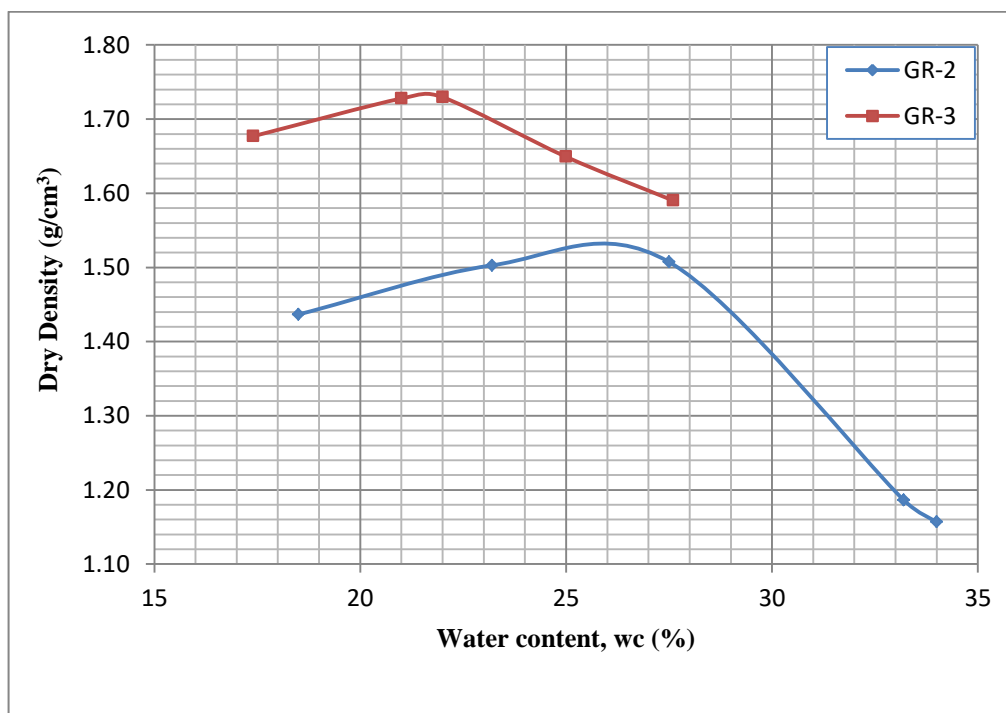


Figure 3.7: Compaction curves for GR-2 and GR-3

3.6 Testing Methods

3.6.1 Standard Oedometer Test, SOT

All tests are carried out by using fixed ring oedometer cell. The initial moisture content is measured as well as final moisture content after the test. The compression and swell are measured by a digital dial gauge using computer programme called DS7 ©2017. This programme is used to record and save the data to a computer in digital format, and manage the testing procedure such as starting and finishing test stages, observing strain- log time curve during the test and monitoring the end of primary consolidation. Immediately after starting the test, distilled water is added to saturate the specimen, after the end of the saturation stage, the loading sequence maintained by applying the following effective stresses in stages of 24 hr (25, 50, 100, 200, 400, 200, 100 and 50 kPa) for soft samples (GR-1). The loading sequences for compacted samples were (25, 50, 100, 200, 400, 800, 400, 200 and 100 kPa).

3.6.2 Creep Test

These test methods cover an experimental investigation of secondary compression behavior of soft samples prepared at various degree of overconsolidation.

For all samples (GR-1) the target preconsolidation stress prior to creep test is attained using static load in the oedometer. In creep test, the samples are saturated under the weight of the loading cap, then preconsolidation stress is applied in once for stresses up to 100 kPa. The preconsolidation stress for greater stresses (200 kPa and 300 kPa) applied in two steps for soft samples, the reason for that is due to that the soil specimens were flowing out of the oedometer cell. After applying preconsolidation

stress the specimens are unloaded for a period 24 hours prior to loading for creep stress.

The compacted samples (GR-2, GR-3) are subjected to dynamic load using standard compaction hammer to apply the preconsolidation stress, hence, the value of preconsolidation stress is calculated from standard oedometer test and then four identical samples are prepared and subjected to an initial preconsolidation stress by also considering the calculation value that obtained from standard oedometer test. The specimens are also allowed for saturation until the end of primary swell is observed and then to calculate preconsolidation stress and the additional stress required to achieve the target OCR is loaded for creep stress.

3.7 Results of Index and Classification Tests

3.7.1. Initial Moisture Content

The in situ moisture content of the clay is measured in the laboratory as 33%.

3.7.2 Particle Size Distribution

Samples are first subjected to wet sieving to evaluate percent passing #200 (75 μm), the percent finer is measured as 97.4%. The results of particle size analysis indicated that the percentage of clay and silt are 54% and 43.4%, respectively, as presented in Figure 3.8. Hence, based on the particle size distribution test results, the soil sample is classified as slightly sandy, silty clay.

3.7.3 Specific Gravity

The specific gravity tests indicated that the particle density of the soil approximately 2.65.

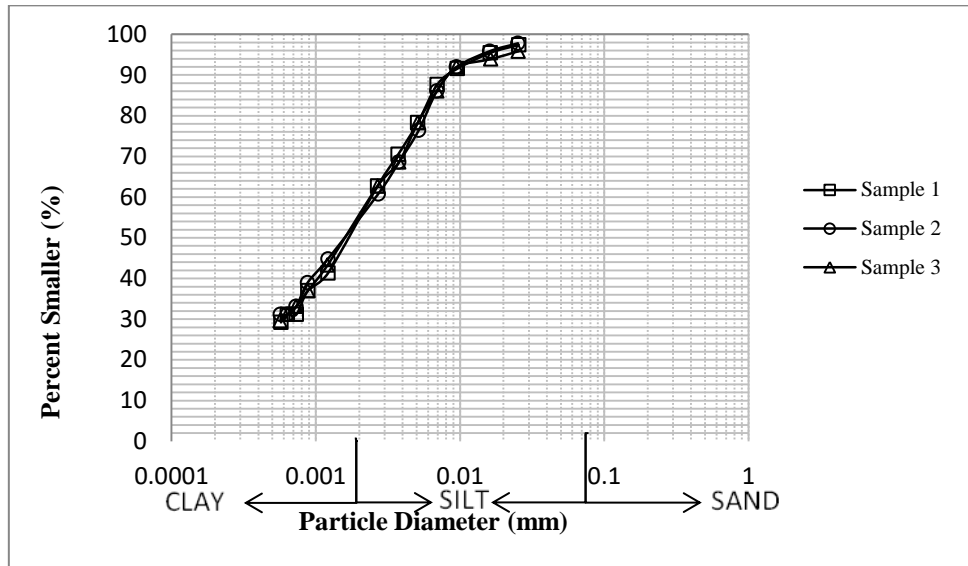


Figure 3.8: Particle size distribution test result

3.7.4 Plasticity Index

The liquid limit is carried out to determine the water content at which the soil transit from plastic state to liquid state. The plastic limit test is carried out to obtain the lowest water content at which the soil is plastic. Two main sample preparation methods are examined as follows:

Natural state method: The soil used in it is natural state without any drying or pulverizing. First, 350 g of soil is mixed with distilled water until the soil worked to a smooth paste then the slurry is placed into a vacuum desiccator for 24 hours. The

results for liquid limit and plastic limit are 61% and 31% respectively. As shown in Figure 3.9.

Drying pulverizing method: The soil is dried in the oven at 50°C for at least five days then pulverized, after that the soil is mixed with distilled water until smooth consistency is observed; next the slurry is kept in a vacuum desiccator for 24 hours. The results for liquid limit and plastic limit tests are 59% and 29% respectively. As shown in Figure 3.10.

Although the results for the two methods are slightly different, the plasticity index is the same ($PI=30$) which does not affect the classification of the soil.

3.7.5 Soil Classification

Based on plasticity tests, when unified classification system is applied the soil can be classified as: High plasticity clay, (CH).

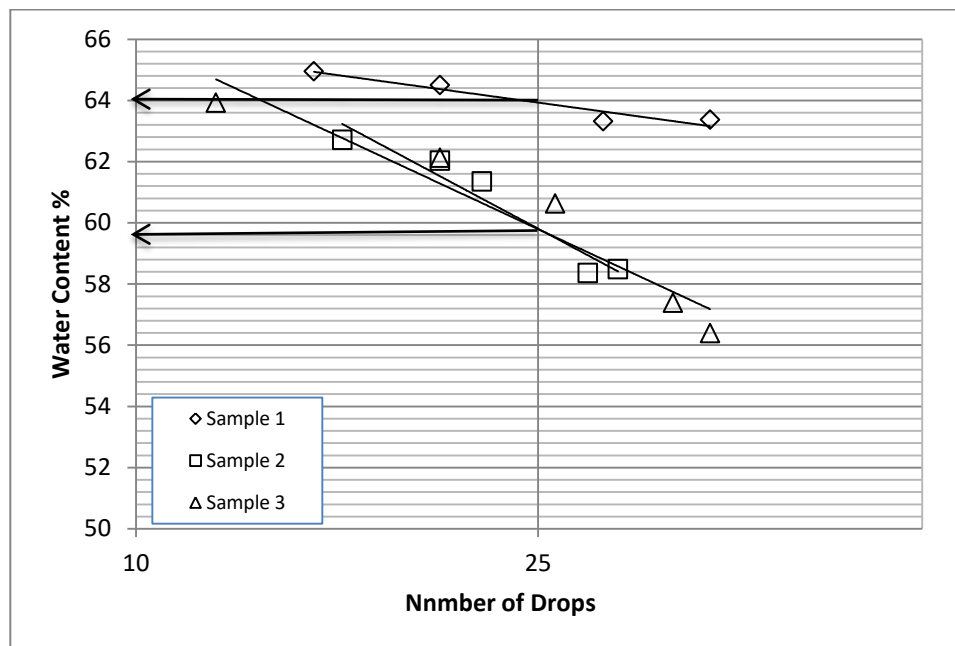


Figure 3.9: Liquid limit test results for natural state method

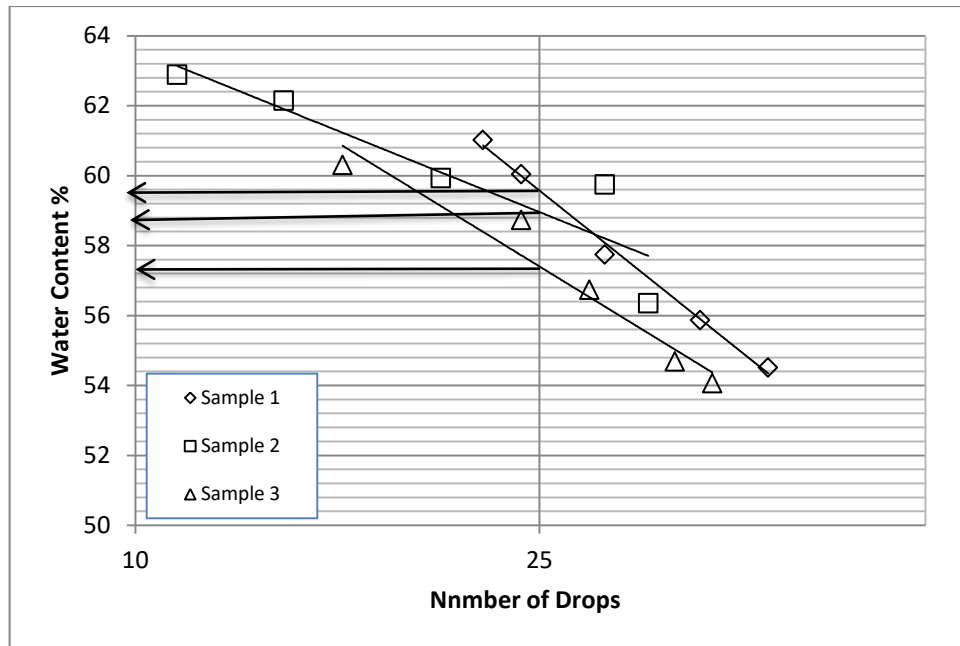


Figure 3.10: Liquid limit test results for drying pulverizing method

Chapter 4

RESULTS, ANALYSIS AND DISCUSSION

4.1 Introduction

In this chapter standard oedometer test and creep test results for soft and compacted samples are presented. The secondary compression behavior of the samples is studied and the results are compared with compressibility characteristics such as

compression index, recompression index, C_r . Furthermore, the test results are compared with the results of the previous studies in the literature.

4.2 Analysis of Compressibility Behavior Using Standard Oedometer Tests

4.2.1 Compression Curves at Each Test Stage

Standard oedometer test was conducted on soft samples and compacted samples. In order to analyze compressibility characteristics, the curves of vertical strain corresponding to the time in logarithmic scale for soft and compacted samples (GR-1, GR-2 and GR-3) are plotted in Figure 4.1 to Figure 4.3. For each test stage the time readings are reset, so that they can be compared to each other on equal grounds.

Initial void ratios of the soft and compacted samples are calculated as 1.59, 0.66 and 0.56 respectively. The soft sample GR-1 has the highest void ratio and the lowest initial void ratio is obtained for the sample prepared with highest compaction energy (GR-3).

As it can be observed in Figure 4.1, the vertical strain curve of saturation stage for soft sample indicates consolidation under the weight of the loading cap rather than swell, which is due to the reason that the soil sample is in an unconsolidated condition due to the absence of any preconsolidation pressure during sample preparation. Hence, the soft sample consolidates slightly even under the weight of loading cap, which applies a modest stress of only 5.2 kPa approximately.

On the other hand, it can be observed from Figure 4.2 and Figure 4.3 that the saturation stage for compacted samples indicates swell under the weight of loading

cap. The vertical strain curve of GR-2 sample indicates lower swell than GR-3 sample. This can be attributed to the fact that GR-2 and GR-3 samples have experienced an initial preconsolidation stress during sample preparation due to applied compaction energy.

In Figure 4.1, the loading curves for soft sample indicate that the maximum compression in the sample is attained in the 25 kPa load increment, which is approximately twice the compression observed in the proceeding load increments 50 kPa, 100 kPa, 200 kPa and 400 kPa.

The vertical strain observed in the rebound curves in unloading stages indicates that the greater the unloading stress the greater the rebound strain will be.

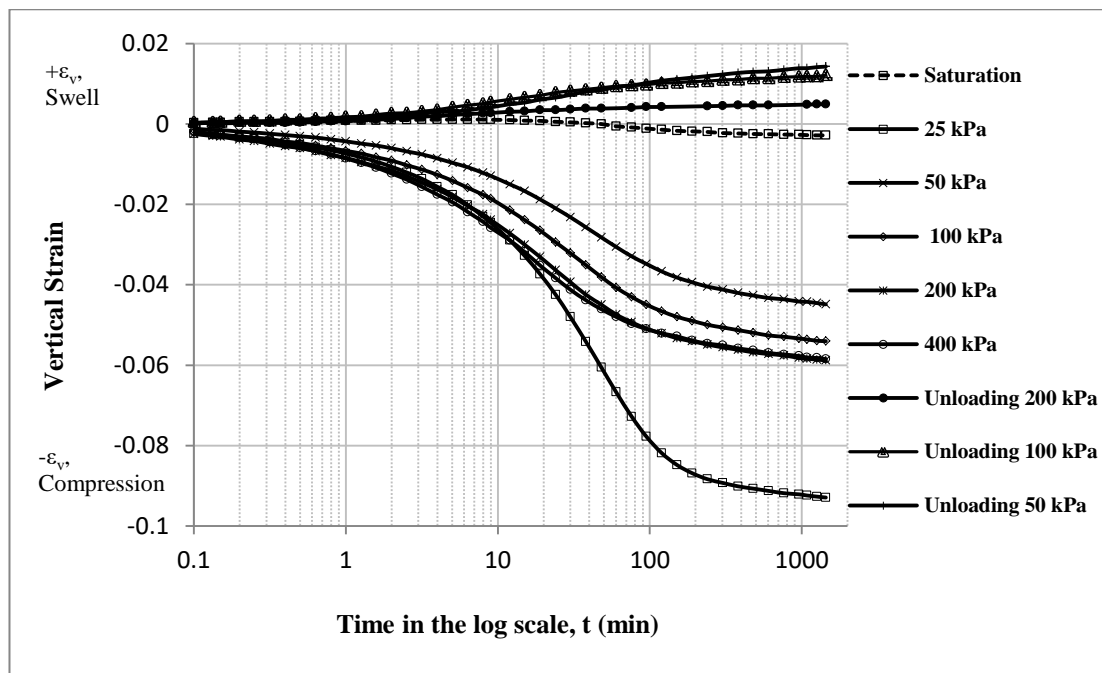


Figure 4.1: Compressibility curves from standard oedometer test, GR-1

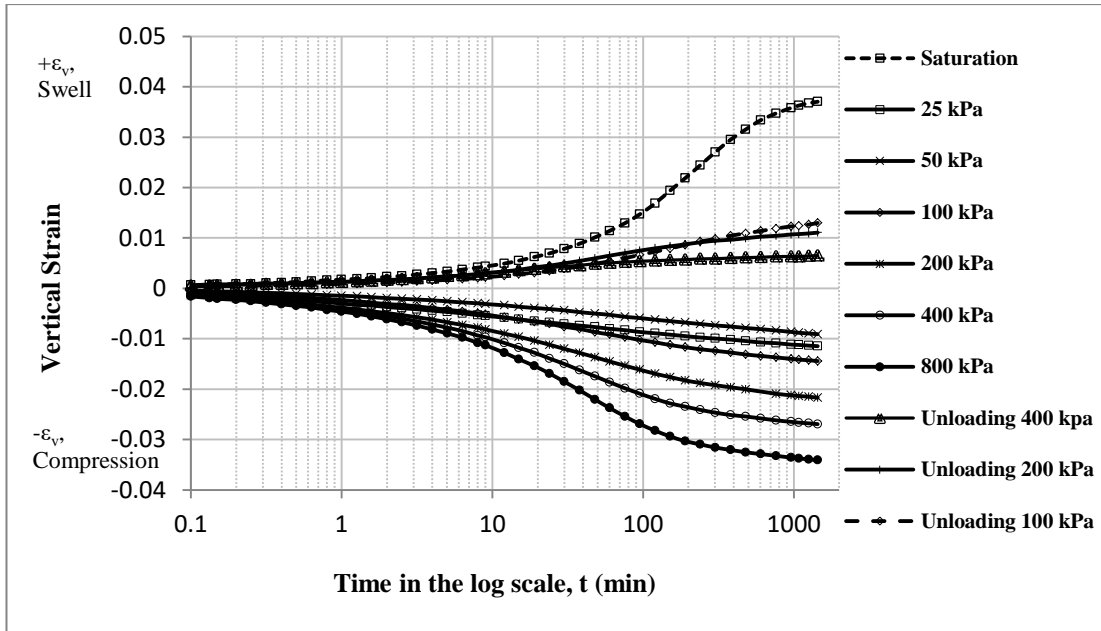


Figure 4.2: Compressibility curves from standard oedometer test, GR-2

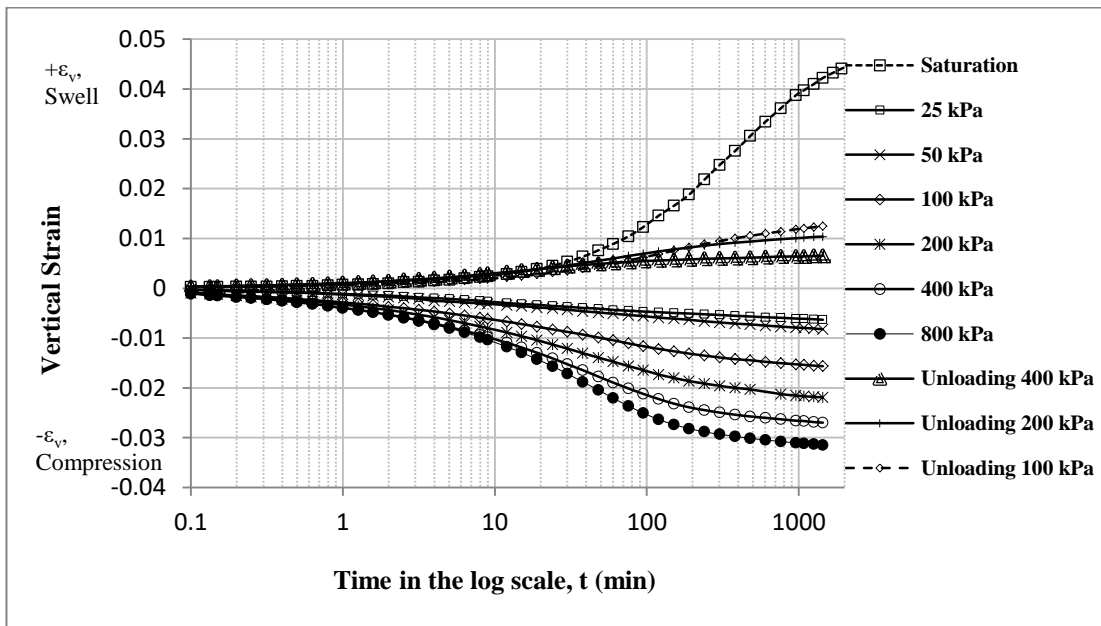


Figure 4.3: Compressibility curves from standard oedometer test, GR-3

4.2.2 Comparison of Compressibility Curves

In Figure 4.4 compressibility curves for soft and compacted samples GR-1, GR-2 and GR-3. The compression curve for soft sample varies linearly in semi-log scale for loading stages; this is considered to be typical of virgin compression behavior due to lack of any pre-stress during sample preparation. However, there is a hump in the

initial part of the compression curves of compacted samples, due to the initial pre-stress induced on the samples during compaction, which might have created preconsolidation in the samples. Therefore, during initial stages of load increments, until this preconsolidation is attained, there is an enhanced resistance in the samples of GR-2 and GR-3 against compression compared to soft sample (GR-1).

The compression curve for soft sample GR-1 shows a greater decrease in void ratio, from 1.58 to 0.93 than compacted samples; void ratios for standard energy GR-2 decreased from about 0.66 to 0.48 and for increased energy GR-3 void ratio reduced from 0.59 to 0.42. In addition, the compression index of the soft sample is 0.4 significantly greater than the compression index for compacted samples (where C_c for GR-2 is 0.12 and for C_c for GR-3 is 0.11). The recompression index for GR-3 is the highest slope observed within all samples with $C_r = 0.0028$, followed by recompression index of GR-2 with $C_r = 0.0018$, and for GR-1 recompression index is obtained as $C_r = 0.0012$. It can be concluded that the recompression index is directly proportional with the compaction energy applied on the sample during sample preparation. The preconsolidation stress is calculated from $(e - \log \sigma'_v)$ curve based on Casagrande's method (Head, 1986); for sample subjected to standard energy, GR-2, the preconsolidation stress is found $P_c = 60$ kPa, and for increased energy, GR-3, it is found as $P_c = 80$ kPa.

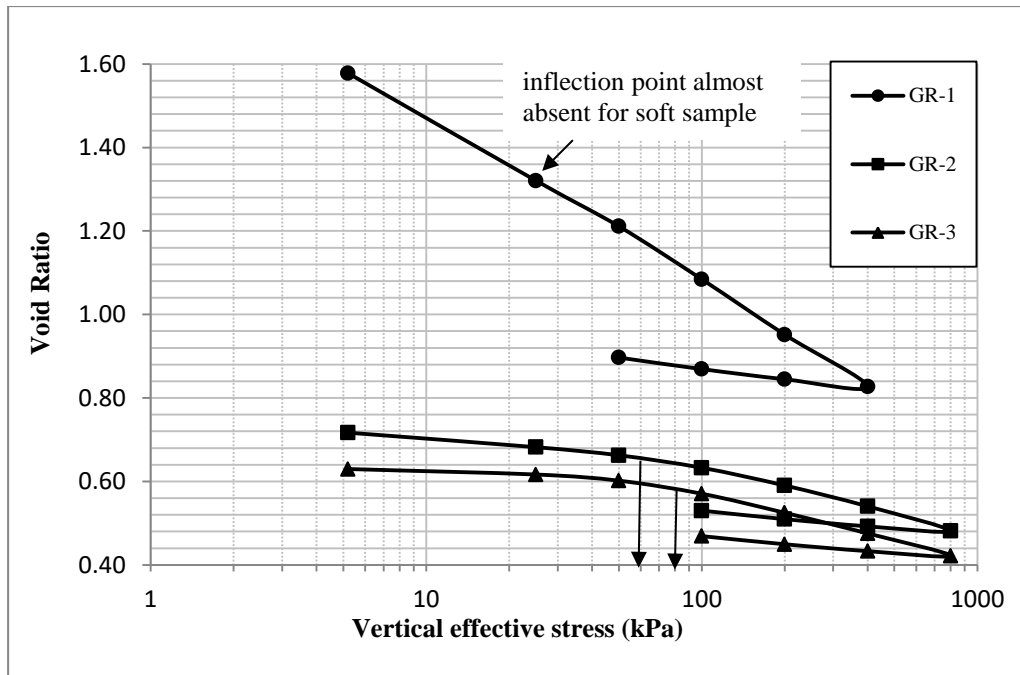


Figure 4.4: Standard oedometer compressibility curves for soft and compacted samples

4.2.3 Analysis of Secondary Compression Behavior Using Standard Oedometer Tests

Figure 4.5 to Figure 4.7 show creep curves obtained from standard oedometer tests for GR-1, GR-2, and GR-3 respectively. After identifying the time corresponding to the end of primary consolidation, the vertical strain versus time data for secondary compression behavior is separated from the primary consolidation curve by resetting the time corresponding to the start of creep as zero. The creep curves for GR-1, GR-2, and GR-3 all indicate an approximately linear trend with log time for all load increments.

It is also observed from the creep curves that, as the effective stress load increased a greater creep strain is obtained for compacted samples of GR-2, and GR-3, with greater creep corresponding to normally consolidated behavior ($\sigma'_v > P_c$).

In Table 4.1 the results of coefficient of secondary compression corresponding to each load stage for soft and compacted samples and also the time corresponding to the end of primary consolidation, t_p for each load stage are presented. From Table 4.1, it is observed that the coefficient of secondary compression is directly proportional with the time corresponding to the end of primary consolidation for all loading stages.

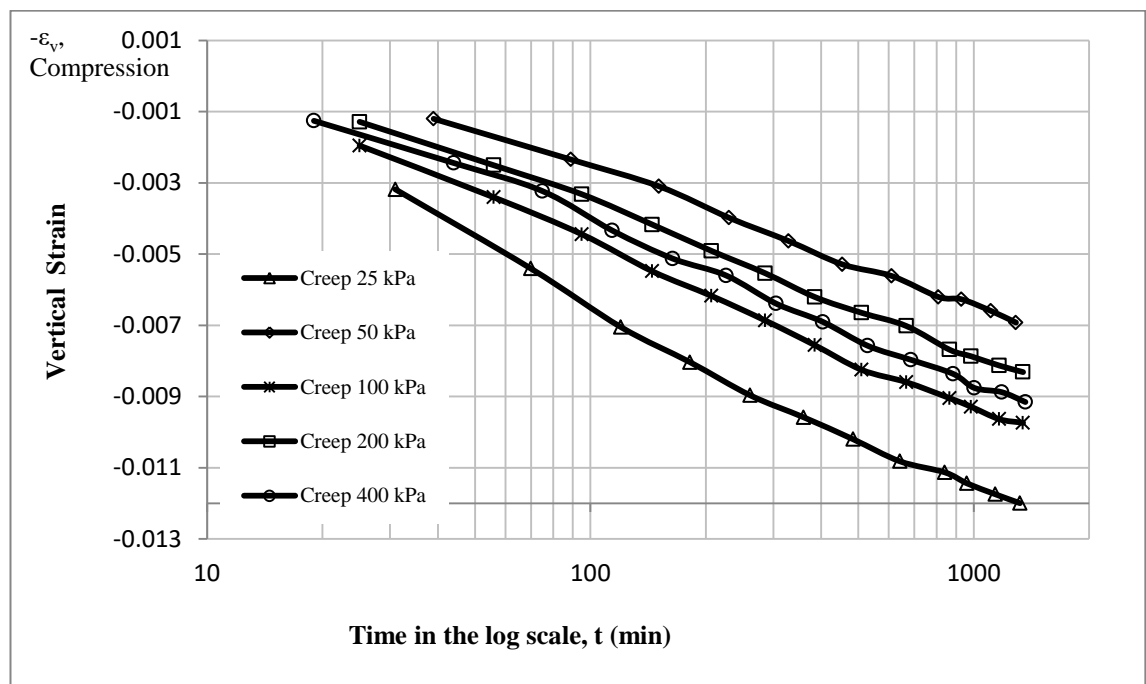


Figure 4.5: Creep curves from standard oedometer test for, GR-1

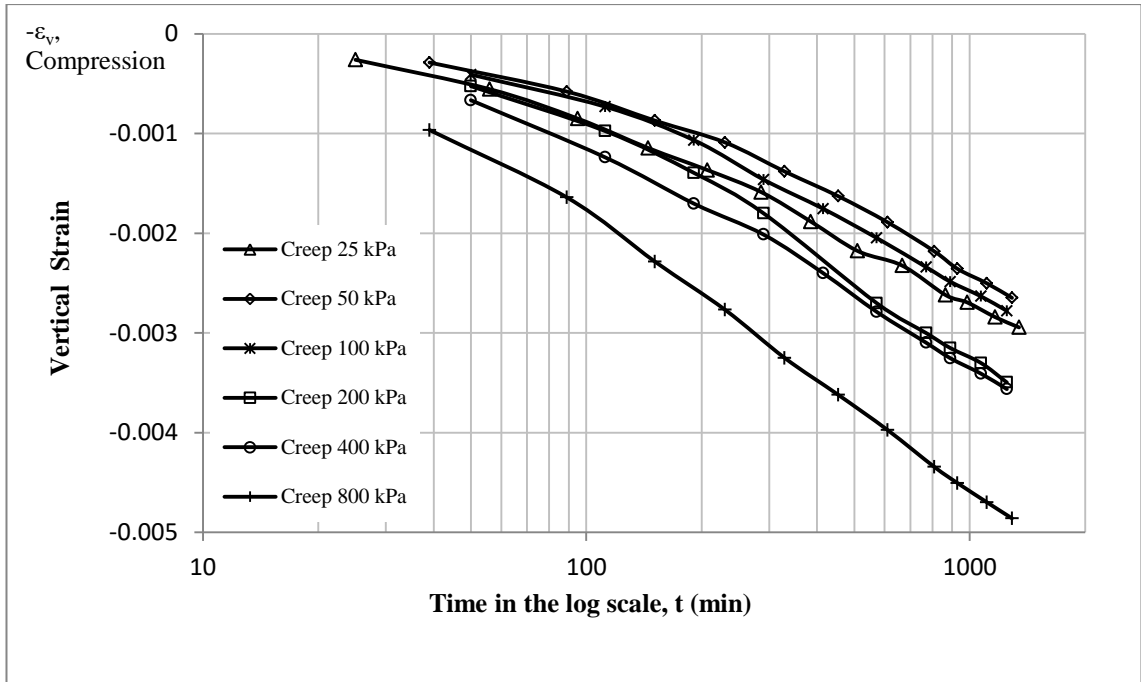


Figure 4.6: Creep curves from standard oedometer test for, GR-2

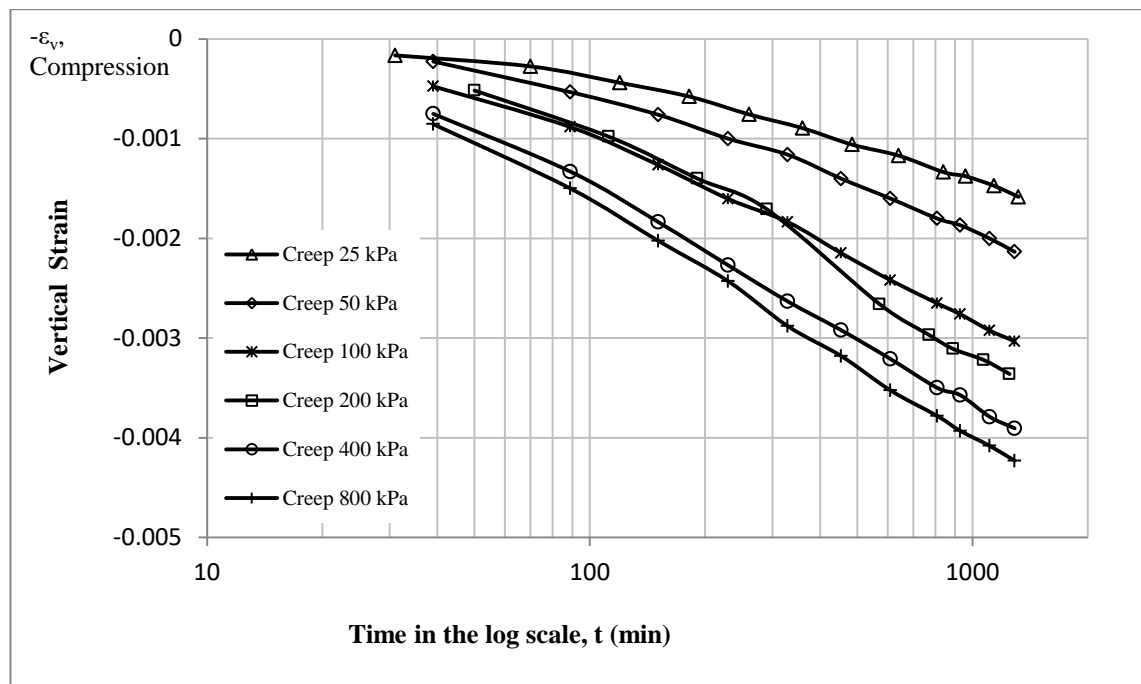


Figure 4.7: Creep curves from standard oedometer test for, GR-3

In Figure 4.8 the relationship between the coefficient of secondary compression and the time corresponding to the end of primary consolidation is presented. In general, the coefficient of secondary compression for soft sample GR-1, is measured to be

greater to the measurements for the compacted samples for all load increments. The time corresponding to the end of primary consolidation for soft sample GR-1 was lower in most of the loading stages compared to measurements for compacted samples. The results of coefficient of secondary compression and the time corresponding to the end of primary consolidation were similar for GR-2 and GR-3, as well as the trends observed.

Table 4.1: Coefficient of secondary compression for soft and compacted samples from standard oedometer tests

σ'_v (kPa)	Soft sample GR-1		Compacted sample GR-2		Compacted sample GR-2	
	$C\alpha$	t_p (min)	$C\alpha$	t_p (min)	$C\alpha$	t_p (min)
25	0.0042	140	0.0010	100	0.0004	120
50	0.0056	160	0.0013	180	0.0014	150
100	0.0045	110	0.0024	220	0.0017	180
200	0.0042	110	0.0031	220	0.0034	200
400	0.0031	80	0.0028	200	0.0028	180
800	-	-	0.0028	180	0.0028	170

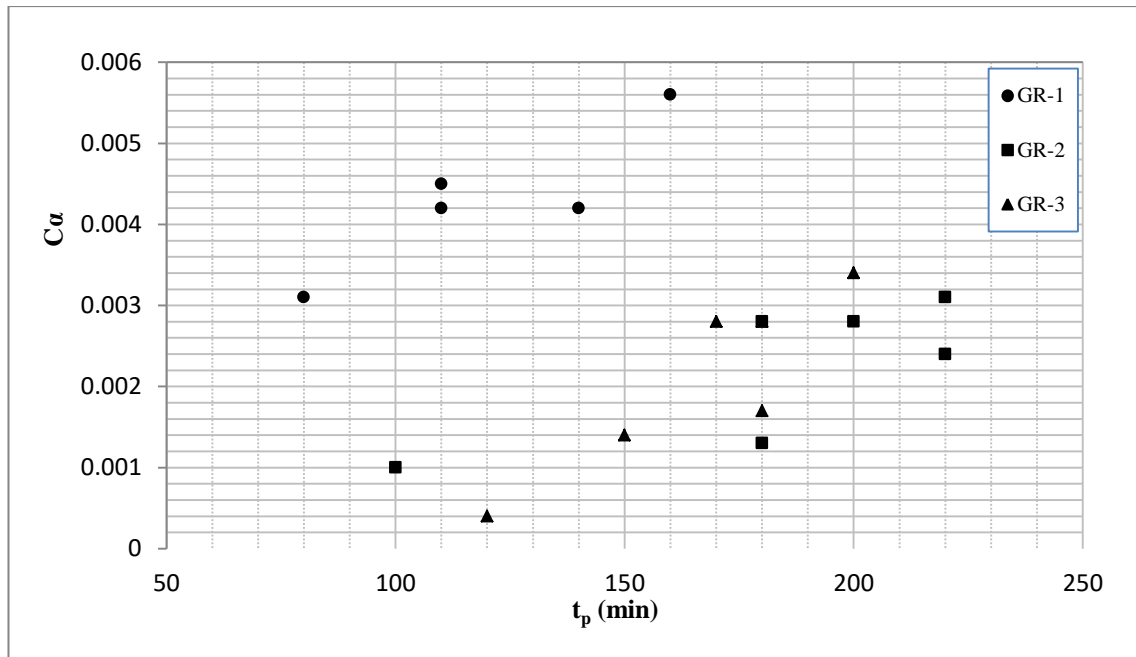


Figure 4.8: Variation of C_α with t_p (min)

Figure 4.9 presents the relationship between the vertical effective stress and the coefficient of secondary compression. It can be observed that the coefficient of secondary compression for soft sample increased from 25 kPa to 50 kPa then gradually decreased with increasing vertical effective stress. On the other hand, the coefficient of secondary compression for compacted samples have similar characteristics, they both increased with increasing vertical effective stress until reaching a peak value around 200 kPa. Then, it decreased and remained constant in the following load increments. The maximum values of the coefficient of secondary compression for compacted samples occur at effective stress about 2.5 times the preconsolidation stress. Similar results for compacted samples were also observed by (Miao and Kavazanjian, 2007) and (Matchala et al., 2008).

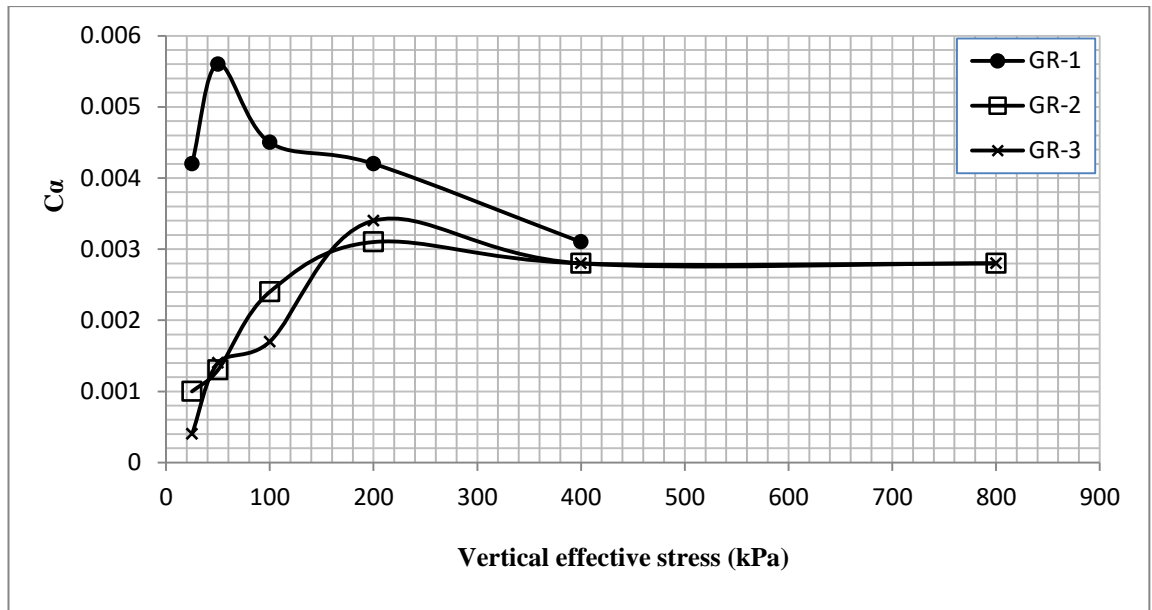


Figure 4.9: Variation of $C\alpha$ with vertical effective stress in standard oedometer tests

4.3 Analysis of Secondary Compression Behavior Using Creep Tests

4.3.1 Assessment of Vertical Strain Curves for Soft Samples

As stated in Chapter 3, there are four sub-groups of soft sample and each sub-group contains four samples which are subjected to the same preconsolidation stress. The data regarding test stages prior to the application of constant effective stress creep tests are plotted in Figure 4.10 to Figure 4.13. These identically prepared and preconsolidated samples are then tested in creep tests under a sustained effective stress to evaluate secondary compression behavior at various overconsolidation ratios; OCR= 1, 1.3, 2, and 4. In this study, the variation of secondary compression behavior with respect to the impact of degree of overconsolidation is also considered.

It can be seen in Figure 4.10 to Figure 4.13 that, the vertical strain curves of saturation and preconsolidation and unloading stages for all samples are almost identical. It is noted that when higher preconsolidation stress is applied, the vertical strain upon unloading is also increased. The relationship observed between

preconsolidation stresses applied and vertical strain upon unloading, obtained after 24 hours are plotted in Figure 4.14.

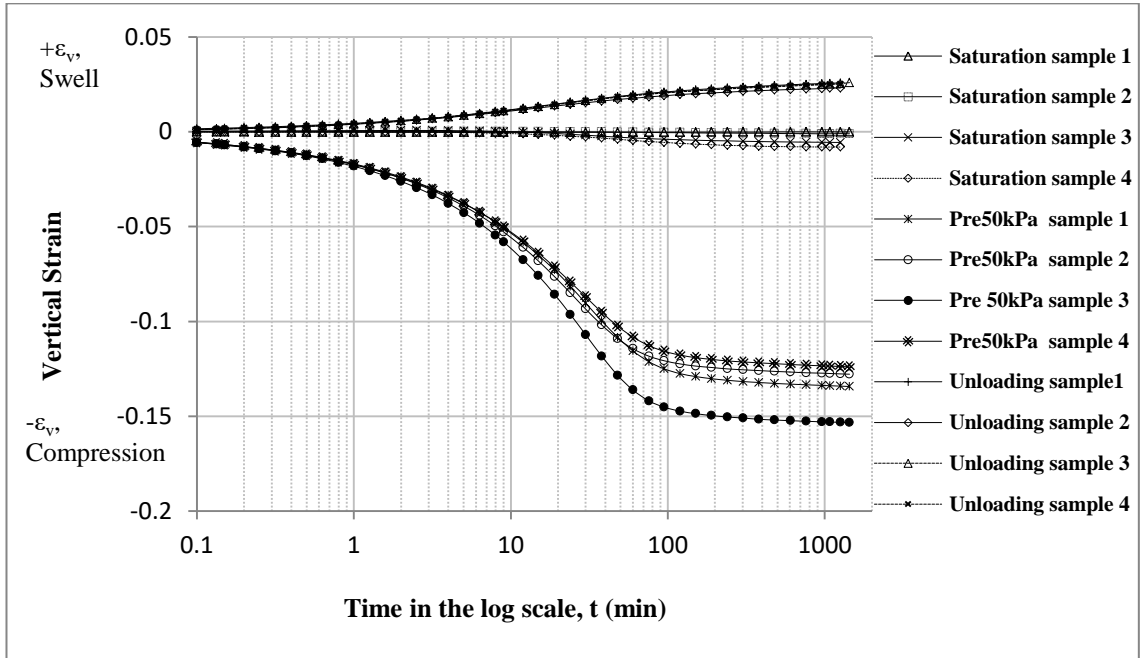


Figure 4.10: Vertical strain curves of GR-1.1 ($P_c=50$ kPa)

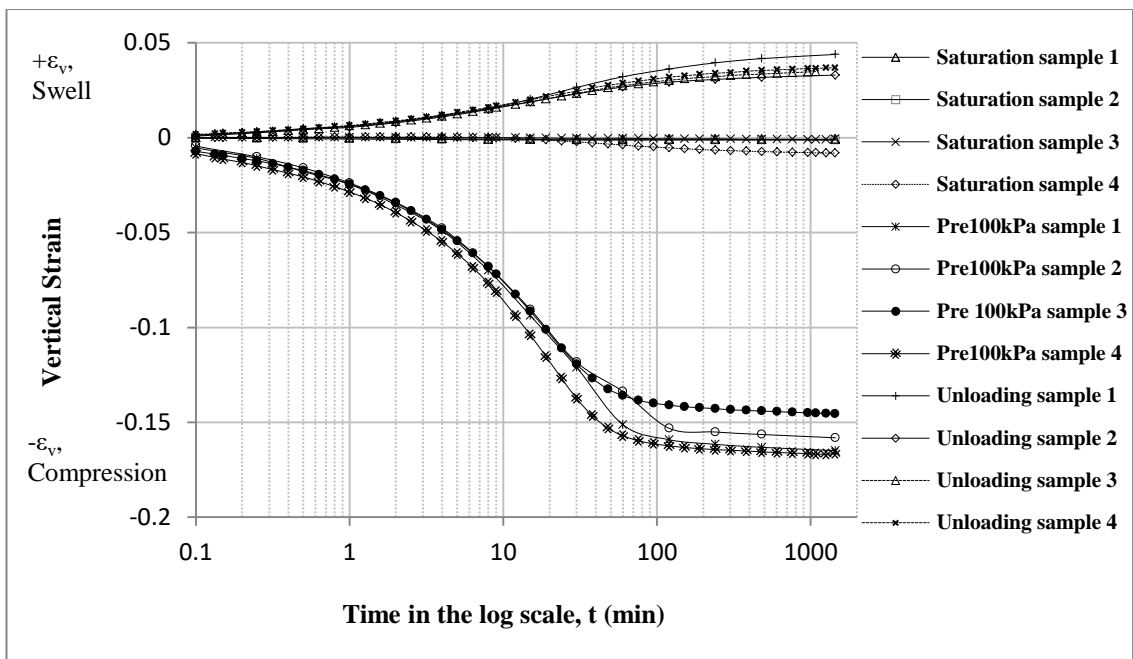


Figure 4.11: Vertical strain curves of GR-1.2 ($P_c=100$ kPa)

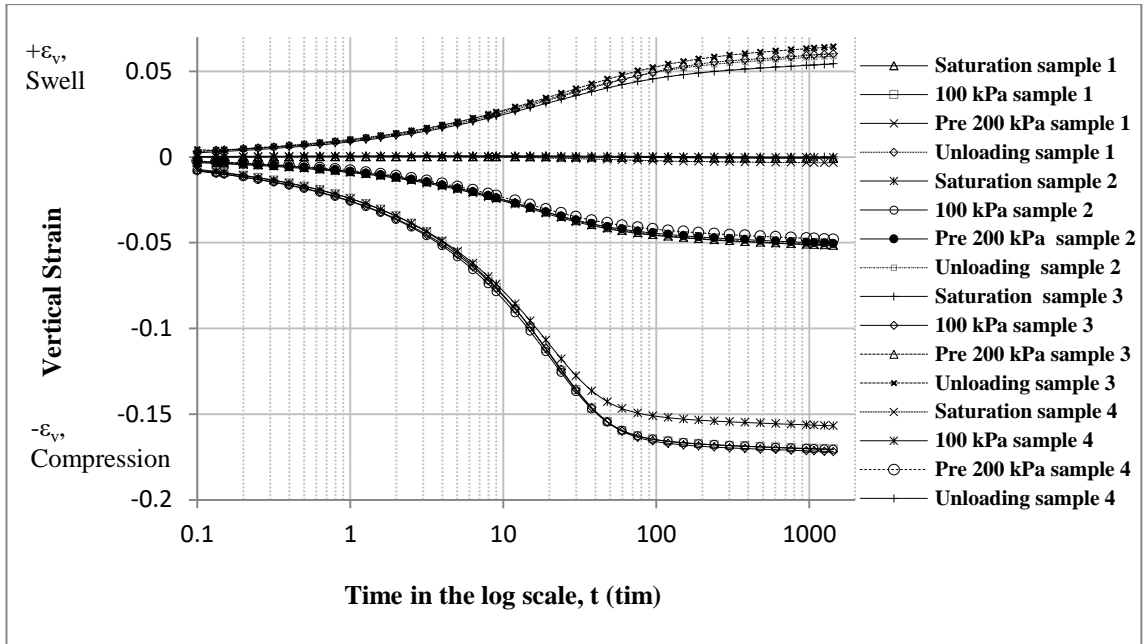


Figure 4.12: Vertical strain curves of GR-1.3 ($P_c=200$ kPa)

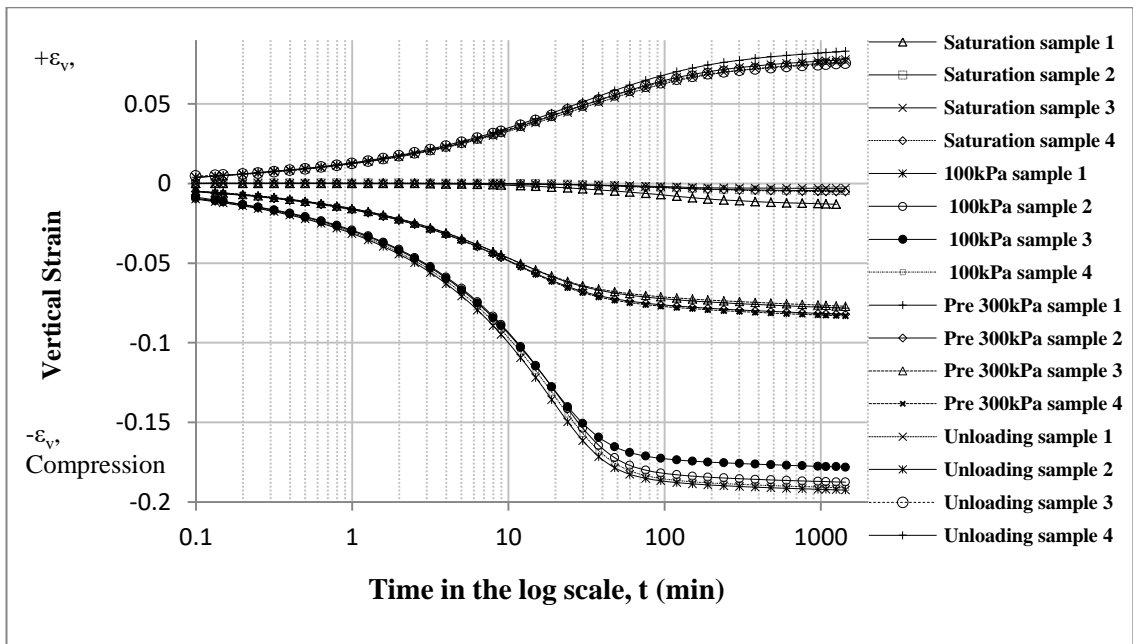


Figure 4.13: Vertical strain curves of GR-1.4 ($P_c=300$ kPa)

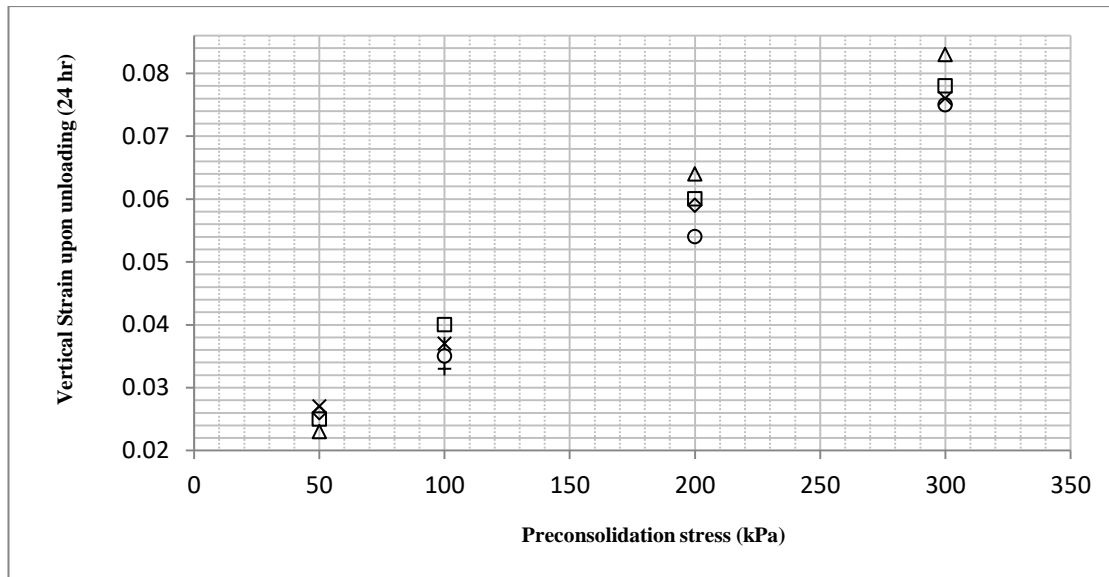


Figure 4.14: The relationship observed between preconsolidation stress and vertical strain upon unloading, obtained after 24 hours

The creep measured with respect to log time at constant effective stress for GR-1.1, GR-1.2, GR-1.3 and GR-1.4 are plotted in Figure 4.15 to Figure 4.18. It is observed that the slope of vertical strain curves are initially greater, and then as time is increased it gradually decreases. In almost all vertical strain curves for samples with highest degree of overconsolidation $OCR=4$ there is a significant decrease in the slope such that the curves are almost asymptotic to the time axis hinting completion of secondary compression.

Vertical strain curves of $OCR=2$ attained greater slopes than $OCR=4$. Likewise, the slopes of vertical strain curves of $OCR=1.3$ are greater than $OCR=2$ and the same relationship obtained between $OCR=2$ and $OCR=1$. Hence, It can be stated that the variation of creep with time strongly depends on OCR . This is in a good conformity with the results observed by (Matchala et al., 2008) and (Luo and Chen, 2014). It should also be stated that while a limiting creep strain is observable for samples with higher degree of overconsolidation, this is almost absent for normally consolidated samples with $OCR=1$.

Fitting curve based on the function proposed by (Yin, 1999) is applied on creep curves in order to compare between the fitting curves and the curves obtained from standard oedometer test. The proposed function is presented in Chapter 2, equation 2.6.

The initial creep time t_0 is obtained from standard oedometer test as proposed by Casagrande (Head, 1986) which is the time corresponding to the end of primary consolidation. Then, the constant parameters $\Delta\epsilon_1$ and ψ_0 is found by using the fundamental method trial and error.

Table 4.2 shows the constant parameters of the function proposed by (Yin, 1999) for soft samples. In Figure 4.15 to Figure 4.18, the best fitting curves and creep curves obtained from creep test of soft samples are plotted. It is found that the proposed function indicate good fitting most of creep curves for soft samples. It is noted that proposed function indicated better fit for samples subjected to higher OCR.

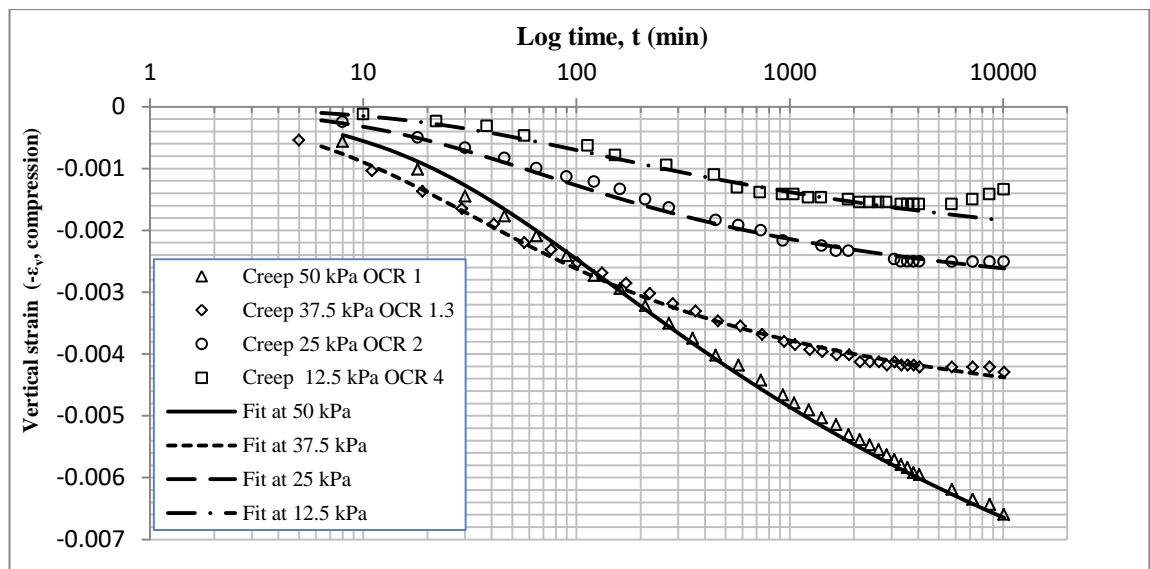


Figure 4.15: Vertical strain creep curves of GR-1.1

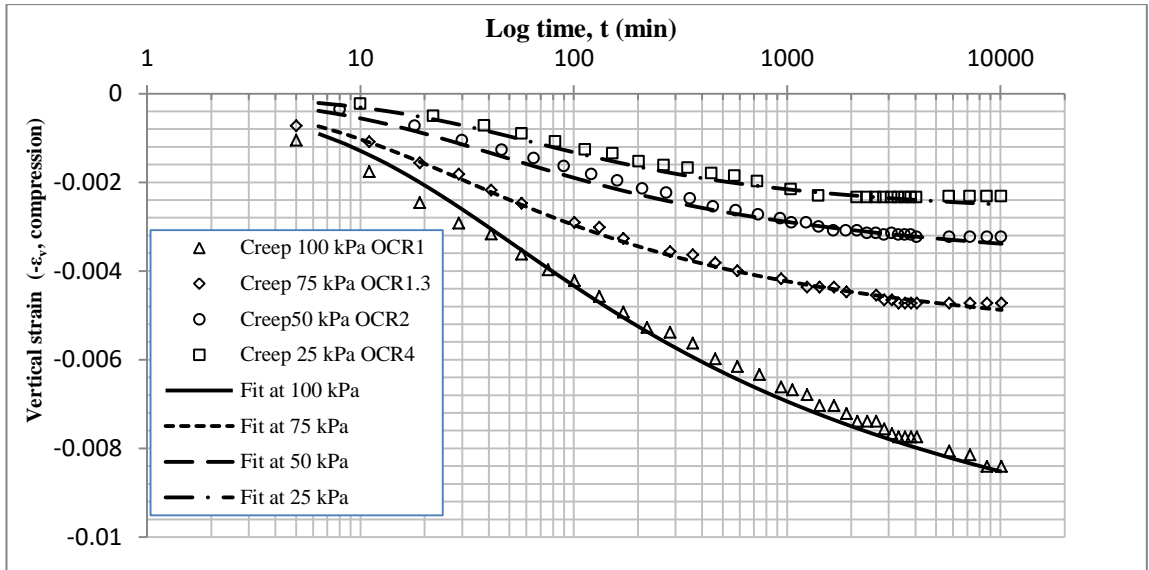


Figure 4.16: Vertical strain creep curves of GR-1.2

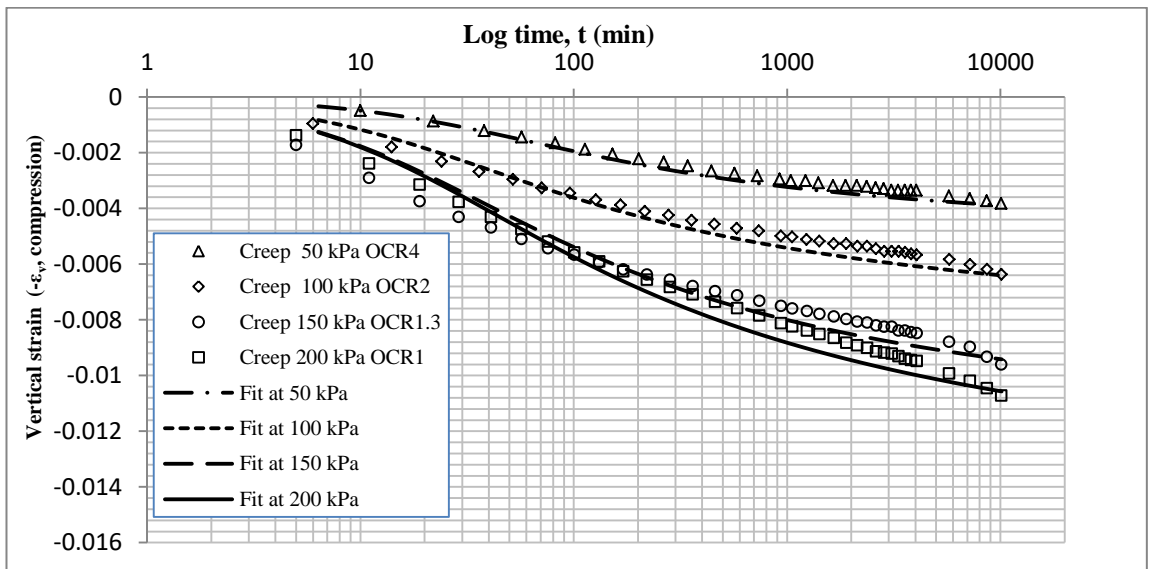


Figure 4.17: Vertical strain creep curves of GR-1.3

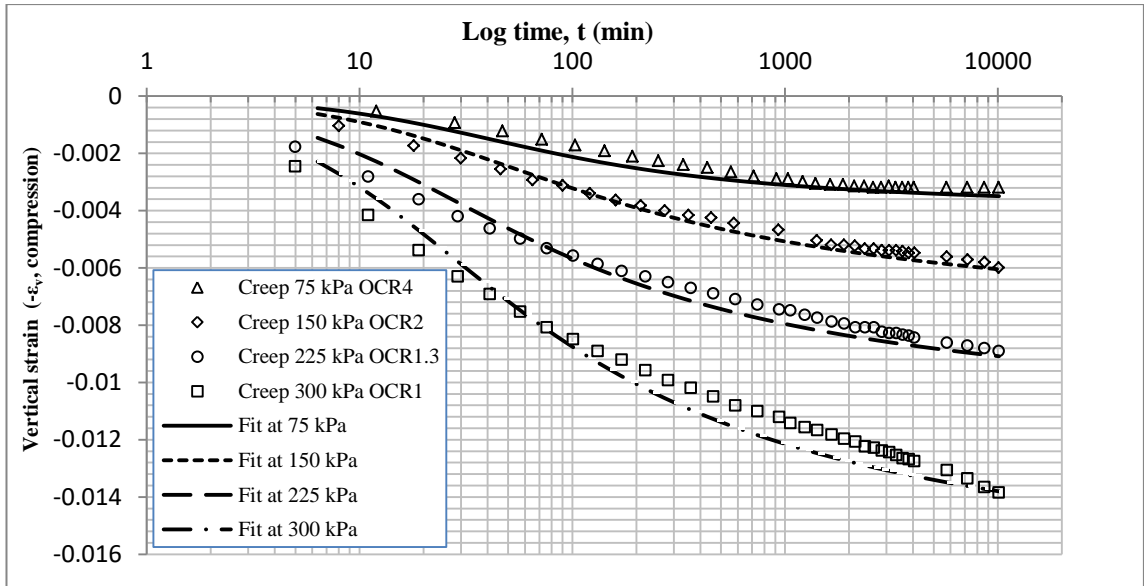


Figure 4.18: Vertical strain creep curves of GR-1.4

Table 4.2: Non linear fitting curve parameters for soft samples.

Group	OCR	Creep load (kPa)	t_p (min)	Ψ_o	$\Delta\epsilon_1$
GR1-1 $P_c=50$ kPa	4	12.5	40	0.0007	0.007
	2	25	35	0.0014	0.0125
	1.3	37.5	20	0.0026	0.006
	1	50	30	0.002	0.0155
GR1-2 $P_c=100$ kPa	4	25	70	0.0026	0.0031
	2	50	30	0.0022	0.0046
	1.3	75	20	0.003	0.0066
	1	100	20	0.0035	0.014
GR1-3 $P_c=200$ kPa	4	50	49	0.0024	0.0055
	2	100	20	0.0033	0.0093
	1.3	150	20	-	-
	1	200	20	-	-

GR1-4 $P_c=300$ kPa	4	75	50	0.0039	0.0042
	2	150	30	0.0035	0.0086
	1.3	225	20	0.006	0.012
	1	300	20	0.0095	0.018

(-) The function did not fit the creep curves.

In this thesis the coefficient of secondary compression is calculated for two consecutive log cycles which provide a. C_α is computed from the slope of the linear segment of the initial part of the curve up 1000 min, then C_{α^*} is computed from the slope of the linear segment of the time interval between 1000 min to 10000 min.

In Table 4.3 the coefficient of secondary compression obtained for soft samples are presented. It can be seen in Table 4.3 that the coefficient of secondary compression C_α is not constant with time on semi logarithmic scale, it decreases from C_α to C_{α^*} .

It is interesting also to note that for OCR= 4 the coefficient of secondary compression C_{α^*} reduced to a very small number such that it may be fair to comment that long term compressibility is almost absent.

The coefficient of secondary compression is observed to be significantly affected from the overconsolidation ratio. The two parameters are observed to be indirectly proportional which is in good agreement with (Mesri and Vardhanabhuti, 2005), (Nurly and Yulindasari, 2007) and (Li et al., 2012).

Table 4.3: Coefficient of secondary compression for soft samples.

Group	OCR	σ'_v kPa	C_α	C_{α^*}
	1	50	0.00241	0.00172
	1.3	37.5	0.00193	0.00028

1-1	2	25	0.00083	0.00014
	4	12.5	0.00069	-
1-2	1	100	0.00211	0.00160
	1.3	75	0.00140	0.00071
	2	50	0.00112	0.00042
	4	25	0.00028	-
1-3	1	200	0.00207	0.00138
	1.3	150	0.00139	0.00104
	2	100	0.00138	0.00069
	4	50	0.00090	0.00055
1-4	1	300	0.00278	0.00139
	1.3	225	0.00208	0.00138
	2	150	0.00138	0.00103
	4	75	0.00104	-

Note: - Calculation could not be performed due to the rate approaching to zero.

4.3.2 Analysis of Secondary Compression of Compacted Samples

The secondary compression behavior for two different groups of compacted samples is investigated, the first group of four samples is subjected to standard compaction energy GR-2, and the preconsolidation stress is computed from standard oedometer test as 60 kPa. The second group is subjected to increased energy GR-3 and the preconsolidation stress computed as 80 kPa.

The secondary compression curves for compacted samples corresponding to various time intervals at constant stress are plotted in Figure 4.19 and Figure 4.20. In general, it is observed that the secondary compression during overconsolidated condition for compacted samples decreases with log time. For OCR= 4 and OCR= 2, the slope of secondary compression curve decreased and became approximately asymptotic to the time axis at the end of the test. A similar relationship between the overconsolidation ratio and creep strain is also observed from compacted samples, which are in a good agreement with the results reported by (Luo and Chen, 2014).

The slope of secondary compression curve for compacted samples is observed to be decreasing in the two consecutive log cycles of 100 min – 1000 min and 1000 min – 10000 min as observed for soft samples. However, the decrease is considerably more remarkable for compacted samples, especially for samples with OCR= 2 and OCR= 4.

The drop is even more pronounced for samples prepared with increased compacted energy (GR-3). It is also interesting to note that the maximum value of the secondary compression is obtained in the time range of 100min-1000min, which also reported by (Fred and Ramesh, 1990).

Table 4.4: Coefficient of secondary compression of the compacted samples.

	GR-2				GR-3		
OCR	σ'_v (kPa)	$C\alpha$	$C\alpha^*$	OCR	σ'_v (kPa)	$C\alpha$	$C\alpha^*$
1	60	0.0024	0.0024	1	80	0.0028	0.0017

1.3	45	0.0021	0.0014	1.3	60	0.0021	0.0010
2	30	0.0019	0.0007	2	40	0.0014	0.0007
4	15	0.0014	0.0006	4	20	0.0012	0.0001

Table 4.5 shows the constant parameters of the function proposed by (Yin, 1999) for compacted samples GR-2 and GR-3.

Table 4.5: Non linear fitting curve parameters for compacted samples.

Group	OCR	Creep load (kPa)	t_p (min)	ψ_o	$\Delta\epsilon_1$
GR2 $P_c=60$ kPa	4	15	90	0.001	0.0074
	2	30	50	0.0014	0.013
	1.3	45	55	0.0022	0.0135
	1	60	90	0.0016	0.013
GR3 $P_c=80$ kPa	4	20	90	0.00083	0.0034
	2	40	70	0.0019	0.009
	1.3	60	80	0.0025	0.0087
	1	80	140	0.003	0.009

Figure 4.19 and Figure 4.20, present the best fitting curves and creep curves obtained from creep test of compacted samples. It is found that the proposed function indicates a good fitting to the measured curves for all compacted samples.

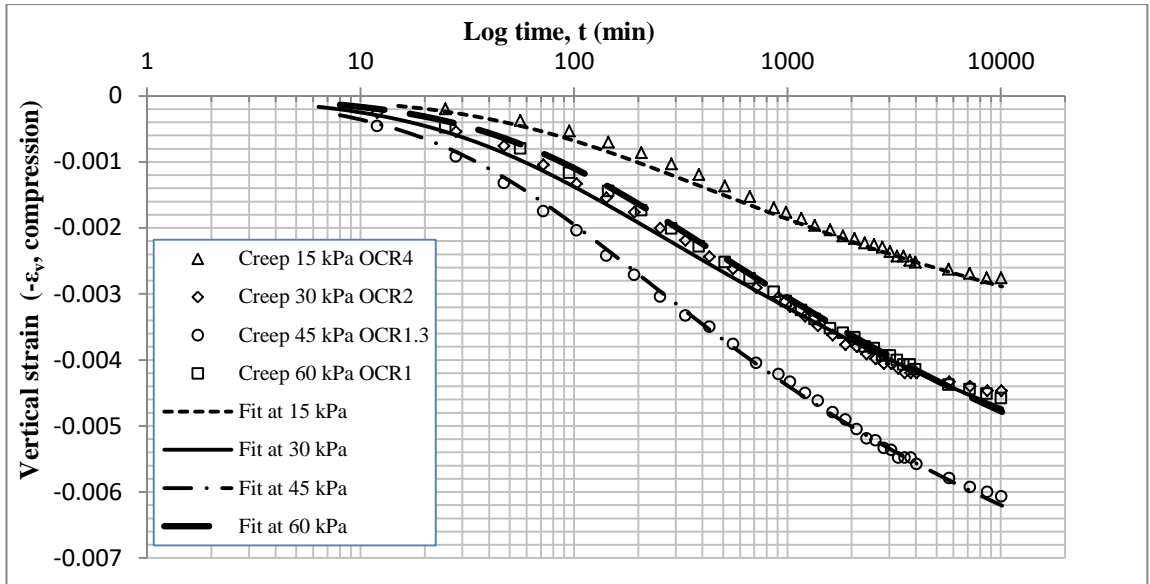


Figure 4.19: Creep curves of compacted samples subjected to standard Energy GR-2

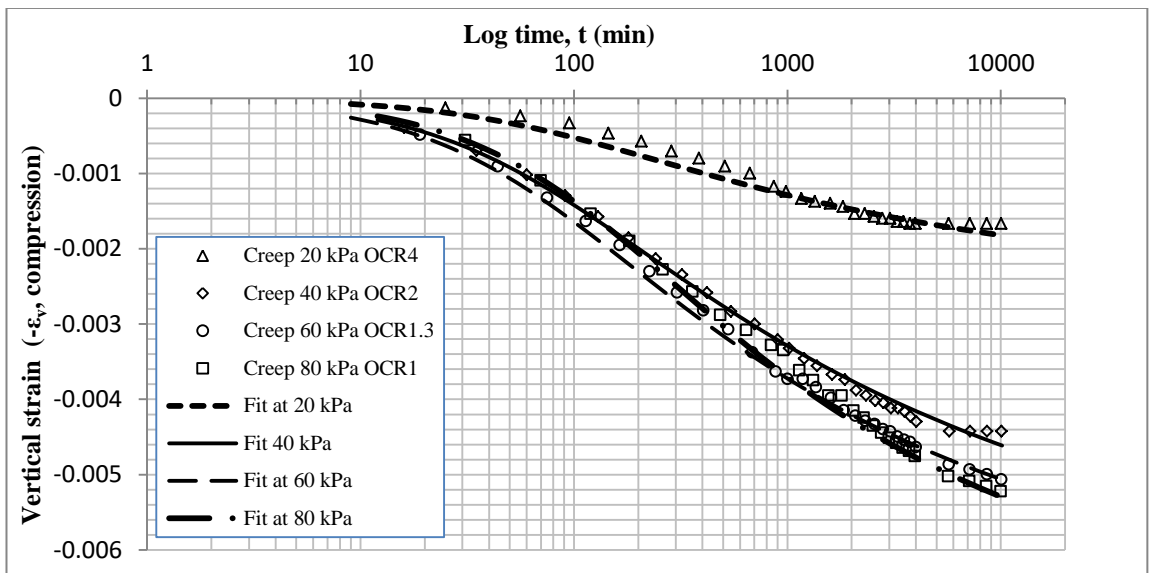


Figure 4.20: Creep curves of compacted samples subjected to increased energy GR-3

4.4 Summarized Critical Review

The coefficient of secondary compression for soft samples increased up to an effective stress of 50 kPa and then gradually decreased. This is similar to the finding by (Li et al. 2012) who reported that coefficient of secondary compression for reconstituted samples increased up to an effective stress of 100 kPa, then gradually decreased to remain constant.

The coefficient of secondary compression for compacted samples increased with increasing vertical effective stress until reaching a peak at vertical effective stress equal to 2.5 times preconsolidation pressure. After this peak, it gradually decreased and remained constant. These results are found in a good agreement with the results reported by (Matchala et al., 2008) and (Miao and Kavazanjian, 2007).

The secondary compression curves decreased with log time for all samples. This is in conformity with the results found by (Luo and Chen., 2014) and (Matchala et al., 2008).

For overconsolidated samples, the coefficient of secondary compression increased with reducing OCR and reached a maximum value at OCR= 1. Similar results are reported by (Mesri and Vardhanabhuti, 2005) and (Nurly and Yulindasari, 2007).

The maximum value of the coefficient of secondary compression occurred in the log time range of 100min to 1000 min for all samples. These results are in line with the results reported by (Fred and Ramesh, 1990).

Calculating the coefficient of secondary compression from standard oedometer test results led to an overestimation of the secondary compression behavior of clay soils.

The function proposed by (Yin, 1999) indicated good fitting to the measured creep curves for all soft and compacted samples using t_0 equal to the time corresponding to the end of primary consolidation.

Chapter 5

CONCLUSION

The importance of this thesis is to gain an understanding of the creep of clay soils.

To establish a better prediction of the long-term settlement of, for example,

embankments or buildings, where measurements of the secondary compression extremely important. In this study, the variation of the secondary compression with time and the effect of the vertical stress on the creep are examined.

From the experimental results of the research carried out on soft and compacted samples to study the behavior of secondary compression during normal and overconsolidated conditions for soft and compacted samples, the following conclusions can be made:

- The method of preparation for soft sample GR-1 considered obtaining identical samples with similar initial void ratio and initial water content.
- Initial void ratios of the soft sample and compacted samples are calculated as 1.59, 0.66 and 0.56 respectively. The soft sample GR-1 has the highest void ratio and the lowest initial void ratio is obtained for the sample prepared with highest compaction energy (GR-3). However, the compression curve for soft sample GR-1 shows a greater decrease in void ratio, from 1.58 to 0.93 than compacted samples; void ratios for standard energy GR-2 decreased from about 0.66 to 0.48 and for increased energy GR-3 void ratio reduced from 0.59 to 0.42.
- The compression index of the soft sample is 0.4 significantly greater than the compression index for compacted samples (where C_c for GR-2 is 0.12 and for C_c for GR-3 is 0.11).
- The vertical strain curve of saturation stage for soft sample indicates consolidation under the weight of the loading cap rather than swell, which is due to the reason that the soil sample is in an unconsolidated condition due to the absence of any preconsolidation pressure during sample preparation. Hence, the soft sample consolidates slightly even under the weight of loading

cap, which applies a modest stress of only 5.2 kPa approximately. On the other hand, the saturation stage for compacted samples indicates swell under the weight of loading cap. The vertical strain curve of GR-2 sample indicates lower swell than GR-3 sample. This can be attributed to the fact that GR-2 and GR-3 samples have experienced an initial preconsolidation stress during sample preparation due to applied compaction energy.

- The loading curves for soft sample indicate that the maximum compression in the sample is attained in the 25 kPa load increment, which is approximately twice the compression observed in the proceeding load increments 50 kPa, 100 kPa, 200 kPa and 400 kPa.
- The vertical strain observed in the rebound curves in unloading stages indicates that the greater the unloading stress the greater the rebound strain will be. The recompression index for GR-3 is the highest slope observed within all samples with $C_r = 0.0028$, followed by recompression index of GR-2 with $C_r = 0.0018$, and for GR-1 recompression index is obtained as $C_r = 0.0012$. The recompression index is directly proportional with the compaction energy applied on the sample during sample preparation.
- The compression curve for soft sample varies linearly in semi-log scale for loading stages; this is considered to be typical of virgin compression behavior due to lack of any pre-stress during sample preparation. However, there is a hump in the initial part of the compression curves of compacted samples, due to the initial pre-stress induced on the samples during compaction, which might have created preconsolidation in the samples. Therefore, during initial stages of load increments, until this preconsolidation is attained, there is an

enhanced resistance in the samples of GR-2 and GR-3 against compression compared to soft sample (GR-1).

- For sample subjected to standard energy, GR-2, the preconsolidation stress is computed as 60 kPa, and for increased energy, GR-3, it is computed as 80 kPa.
- The creep curves obtained from standard oedometer test for GR-1, GR-2, and GR-3 all indicate an approximately linear trend with log time for all load increments. It is also observed from the creep curves that, as the effective stress load increased a greater creep strain is obtained for compacted samples of GR-2, and GR-3, with greater creep corresponding to normally consolidated behavior ($\sigma'_v > P_c$).
- The coefficient of secondary compression is directly proportional with the time corresponding to the end of primary consolidation for all loading stages.
- The coefficient of secondary compression for soft sample increased from 25 kPa to 50 kPa then gradually decreased with increasing vertical effective stress. On the other hand, the coefficient of secondary compression for compacted samples have similar characteristics, they both increased with increasing vertical effective stress until reaching a peak value around 200 kPa. Then, it decreased and remained constant in the following load increments. The maximum values of the coefficient of secondary compression for compacted samples occur at effective stress about 2.5 times the preconsolidation stress.
- As much higher preconsolidation stress maintained on the samples, the vertical unloading strain increased. In which the sample prepared with

increase energy indicated higher unloading vertical strain curve than standard energy.

- During normal consolidated stage the coefficient of secondary compression for soft sample GR-1, is measured to be greater to the measurements for the compacted samples for all load increments. The time corresponding to the end of primary consolidation for soft sample GR-1 was lower in most of the loading stages compared to measurements for compacted samples. The results of coefficient of secondary compression and the time corresponding to the end of primary consolidation were similar for GR-2 and GR-3, as well as the trends observed.
- For overconsolidated samples, the coefficient of secondary compression increased with reducing OCR and reached a maximum value at OCR= 1.
- The coefficient of secondary compression C_{α} is not constant with time on semi logarithmic scale, it decreases from C_{α} to C_{α}^* .
- For OCR= 4 the coefficient of secondary compression C_{α}^* reduced to a very small number such that it may be fair to comment that long term compressibility is almost absent.
- Calculating the coefficient of secondary compression from standard oedometer test results led to an overestimation of the secondary compression behavior of clay soils.
- The proposed function by Yin (1999) indicates good fitting to the measured creep curves at t_p found by oedometer test for all soft samples. It is noted that proposed function indicated better fit for samples subjected to higher OCR.

- For compacted samples, it is found that the proposed function by Yin (1999) indicates a good fitting to the measured creep curves for all compacted samples.

REFERENCES

Al-Shamrani, M. A. (1998). Application of the C_u/C_c concept to secondary compression of Sabkha soils. *Canadian Geotechnical Journal*, 35(1), 15-26.

- Al-Shamrani, M. A., & Dhowian, A. W. (1996). Characterization of secondary compression behavior of Sabkha soils. *Engineering Geology*, 48(1-2), 19-41.
- Atalar, C., & Das, B. M. (2009). Geotechnical properties of Nicosia soils, Cyprus. *Proceedings, 2th Int. Con. New Developments in SMG Eng.*, 360-367, Nicosia.
- Barden, L. (1968). Primary and secondary consolidation of clay and peat. *Geotechnique*, 18(1), 1-24.
- Barden, L. (1969). Time dependent deformation of normally consolidated clays and peats. *Journal of Soil Mechanics & Foundations Div*, 95(1), 1-32.
- Bjerrum, L. (1967). Progressive failure in slopes of overconsolidated plastic clay and clay shales. *Journal of Soil Mechanics & Foundations Div*. 93(5), 1-49.
- Burland, J. B. (1990). On the compressibility and shear strength of natural clays. *Géotechnique*, 40(3), 329-378.
- Craig, R. F. (2004). *Soil mechanics*. London, Spon Press, 447.
- Das, B.M. (2008). *Advanced soil mechanics*. London, Taylor and Francis, 594.
- Deng, Y. F., Cui, Y. J., Tang, A. M., Li, X. L., & Sillen, X. (2012). An experimental study on the secondary deformation of Boom clay. *Applied Clay Science*, 59, 19-25.

- Edgell, C. J., McDonald, C. C., & Graham, J. B. (1983). Permanent cell line expressing human factor VIII-related antigen established by hybridization. *Proceedings of the National Academy of Sciences*, 80(12), 3734-3737.
- Fatahi, B., Le, T. M., Le, M. Q., & Khabbaz, H. (2013). Soil creep effects on ground lateral deformation and pore water pressure under embankments. *Geomechanics and Geoengineering*, 8(2), 107-124.
- Fox, P. J., Edil, T. B., & Lan, L. T. (1992). C_u/C_c Concept applied to compression of peat. *Journal of Geotechnical Engineering*, 118(8), 1256-1263.
- Gofar, N., & Sutejo, Y. (2007). Long-term compression behavior of fibrous peat. *Malaysian Journal of Civil Engineering*, 19(2), 104-116.
- Head, K. H., & Epps, R. (1986). *Manual of soil laboratory testing* (Vol (3), 798-869). London: Pentech Press.
- Lei, H., Wang, X., Chen, L., Huang, M., & Han, J. (2016). Compression characteristics of ultra-soft clays subjected to simulated staged preloading. *KSCE Journal of Civil Engineering*, 20(2), 718-728.
- Leroueil, S., Kabbaj, M., Tavenas, F., & Bouchard, R. (1985). Stress–strain–strain rate relation for the compressibility of sensitive natural clays. *Geotechnique*, 35(2), 159-180.

- Li, Q., Ng, C. W. W., & Liu, G. B. (2012). Low secondary compressibility and shear strength of Shanghai Clay. *Journal of Central South University*, 19(8), 2323-2332.
- Luo, Q., & Chen, X. (2014). Experimental research on creep characteristics of Nansha soft soil. *The Scientific World Journal*, 2014 :968738. doi:10.1155/2014/968738
- Malekzadeh, M., & Bilsel, H. (2012). Swell and compressibility of fiber reinforced expansive soils. *International Journal of Advanced Technology in Civil Engineering*, 1(2), 42-45.
- Mesri, G., & Castro, A. (1987). C_a/C_c concept and K_0 during secondary compression. *Journal of Geotechnical Engineering*, 113(3), 230-247.
- Mesri, G., Kelly, W. E., Vallee, R. P., & Andersland, O. B. (1973). Coefficient of secondary compression. *Journal of Soil Mechanics & Foundations Div*, 99.(Proc Paper).
- Mesri, G., Stark, T. D., Ajlouni, M. A., & Chen, C. S. (1997). Secondary compression of peat with or without surcharging. *Journal of Geotechnical and Geoenvironmental Engineering*, 123(5), 411-421.
- Mesri, G., & Vardhanabhuti, B. (2006). Closure to "Secondary Compression". *Journal of Geotechnical and Geoenvironmental Engineering*, 132(6), 817-818.

- Miao, L., & Kavazanjian Jr, E. (2007). Secondary compression features of Jiangsu soft marine clay. *Marine Georesources and Geotechnology*, 25(2), 129-144.
- Nash, D. F. T., Sills, G. C., & Davison, L. R. (1992). One-dimensional consolidation testing of soft clay from Bothkennar. *Geotechnique*, 42(2), 241-256.
- Sridharan, A., & Prakash, K. (1998). Characteristic water contents of a fine-grained soil-water system. *Geotechnique*, 48(3), 337-346.
- Sridharan, A., & Rao, A. S. (1982). Mechanisms controlling the secondary compression of clays. *Geotechnique*, 32(3), 249-260.
- Suneel, M., Park, L. K., & Im, J. C. (2008). Compressibility characteristics of Korean marine clay. *Marine Georesources and Geotechnology*, 26(2), 111-127.
- Tawfiq, S., & Nalbantoglu, Z. (2009, May). Swell-Shrink behavior of expansive clays. *In Proceedings of 2nd International Congress on New Developments in Soil Mechanics and Geotechnical Engineering, Nicosia, North Cyprus*, 336-341.
- Terzaghi, K., Peck, R. B., & Mesri, G. (1996). *Soil mechanics in engineering practice*. John Wiley & Sons.
- Walker, L. K. (1969). Undrained creep in a sensitive clay. *Geotechnique*, 19(4), 515-529.

Yin, J. H. (1999). Non-linear creep of soils in oedometer tests. *Geotechnique*, 49(5), 699-707.

Zeng, L., & Liu, S. (2010). A calculation method of secondary compression index for natural sedimentary clays using void index. *In Soil Behavior and Geomicromechanics*, 14-21.

APPENDICES

Appendix A: Test Reports for Standard Oedometer Tests

1- Standard Oedometer Test

Table A1.1 Standard oedometer test report for GR-1

Starting date	24/3/2017	
Finishing date	1/4/2017	
Consolidation type =	Fixed ring consolidometer	
Before test		
Mass of the ring(g)	61.44	
Inside diameter of the ring (cm)	4.98	
Height of specimen, H_i (cm)	1.44	
Area of specimen, A (cm ²)	19.48	
Mass of specimen + ring (g)	107.96	
Initial moisture content of specimen, w_i (%)	62	
Specific gravity of solids, G_s	2.65	
After test		
Mass of wet sample + ring(g)	100.97	
Mass of can(g)	71.56	
Mass of can + wet soil (g)	77.01	
Mass of wet specimen (g)	39.53	
Mass of can + dry soil (g)	75.51	
Mass of dry specimen, M_d (g)	28.65	
Final moisture content of specimen, w_f %	38	
Calculations		
Mass of solids in specimen, M_d (g)		28.6502
Mass of water in specimen before test, M_{wi} (g)	$W_i \times M_d$	17.7631
Mass of water in specimen after test, M_{wf} (g)	$W_f \times M_d$	10.8798
ρ_w		1 g/cm ³
Height of solids, H_s (cm)	$M_d / (A \cdot G_s \cdot \rho_w)$	0.55505
Height of water before test, H_{wi} (cm)	$M_{wi} / (A \cdot \rho_w)$	0.9119
Height of water after test, H_{wf} (cm)	$M_{wf} / (A \cdot \rho_w)$	0.5586
$\Sigma \Delta H$ (cm)		0.382184
Height of specimen after test, (cm)		1.0528
Void ratio before test, e_o	$(H_i - H_s) / H_s$	1.5853
Void ratio after test, e_f	$(H_f - H_s) / H_s$	0.8968

Table A1.2 Standard oedometer test report for GR-2

Starting date	30/5/2017	
Finishing date	11/6/2017	
Consolidation type =	Fixed ring consolidometer	
Before test		
Mass of the ring(g)	61.66	
Inside diameter of the ring (cm)	4.97	
Height of specimen, H_i (cm)	1.44	
Area of specimen, A (cm ²)	19.42	
Mass of specimen + ring (g)	118.76	
Initial moisture content of specimen, w_i (%)	27	
Specific gravity of solids, G_s	2.65	
After test		
Mass of wet sample + ring(g)	118.81	
Mass of can(g)	82.70	
Mass of can + wet soil (g)	94.90	
Mass of wet specimen (g)	57.15	
Mass of can + dry soil (g)	92.24	
Mass of dry specimen, M_d (g)	44.69	
Final moisture content of specimen, w_f %	28	
Calculations		
Mass of solids in specimen, M_d (g)		44.6894
Mass of water in specimen before test, M_{wi} (g)	$W_i \times M_d$	12.2002
Mass of water in specimen after test, M_{wf} (g)	$W_f \times M_d$	12.4606
ρ_w		1 g/cm ³
Height of solids, H_s (cm)	$M_d / (A * G_s * \rho_w)$	0.86857
Height of water before test, H_{wi} (cm)	$M_{wi} / (A * \rho_w)$	0.6284
Height of water after test, H_{wf} (cm)	$M_{wf} / (A * \rho_w)$	0.6418
$\Sigma \Delta H$ (cm)		0.1089761
Height of specimen after test, (cm)		1.3290
Void ratio before test, e_o	$(H_i - H_s) / H_s$	0.6556
Void ratio after test, e_f	$(H_f - H_s) / H_s$	0.5301

Table A1.3 Standard oedometer test report for GR-3

Starting date	30/5/2017	
Finishing date	11/6/2017	
Consolidation type =	Fixed ring consolidometer	
Before test		
Mass of the ring(g)	61.19	
Inside diameter of the ring (cm)	4.97	
Height of specimen, H_i (cm)	1.45	
Area of specimen, A (cm ²)	19.40	
Mass of specimen + ring (g)	120.54	
Initial moisture content of specimen, w_i (%)	23.40	
Specific gravity of solids, G_s	2.65	
After test		
Mass of wet sample + ring(g)	121.74	
Mass of can(g)	49.81	
Mass of can + wet soil (g)	61.34	
Mass of wet specimen (g)	60.55	
Mass of can + dry soil (g)	58.95	
Mass of dry specimen, M_d (g)	48.00	
Final moisture content of specimen, w_f %	0.26	
Calculations		
Mass of solids in specimen, M_d (g)		47.9989
Mass of water in specimen before test, M_{wi} (g)	$W_i \times M_d$	1123.1736
Mass of water in specimen after test, M_{wf} (g)	$W_f \times M_d$	12.5511
ρ_w		1 g/cm ³
Height of solids, H_s (cm)	$M_d / (A \cdot G_s \cdot \rho_w)$	0.93365
Height of water before test, H_{wi} (cm)	$M_{wi} / (A \cdot \rho_w)$	57.8954
Height of water after test, H_{wf} (cm)	$M_{wf} / (A \cdot \rho_w)$	0.6470
$\Sigma \Delta H$ (cm)		0.0804
Height of specimen after test, (cm)		1.3716
Void ratio before test, e_o	$(H_i - H_s) / H_s$	0.5552
Void ratio after test, e_f	$(H_f - H_s) / H_s$	0.4691

2 . Vertical Strain and Void Ratio Calculation

Table A2.1 Values of vertical strain and void ratio for each load stage for GR-1

Vertical stress Kpa	ΔH	Specimen Height H(mm)	Vertical strain (%)	Void ratio
5.2	0.0404	14.3096	0.2815	1.5781
25	1.4698	12.8802	10.2422	1.3206
50	2.0766	12.2734	14.4708	1.2112
100	2.7807	11.5693	19.3779	1.0844
200	3.5168	10.8332	24.5075	0.9517
400	4.2097	10.1403	29.3357	0.8269
200	4.1099	10.2401	28.6404	0.8449
100	3.9754	10.3746	27.7029	0.8691
50	3.8218	10.5282	26.6330	0.8968

Table A2.2 Values of vertical strain and void ratio for each load stage for GR-2

Vertical stress Kpa	ΔH	Specimen Height H(mm)	Vertical strain (%)	Void ratio
5.2	-0.5325	14.9125	-3.7029	0.7169
25	-0.2305	14.6105	-1.6027	0.6821
50	-0.0620	14.4420	-0.4310	0.6627
100	0.1976	14.1824	1.3741	0.6328
200	0.5664	13.8136	3.9387	0.5904
400	1.0005	13.3795	6.9574	0.5404
800	1.5141	12.8659	10.5291	0.4813
400	1.4163	12.9637	9.8492	0.4925
200	1.2666	13.1134	8.8078	0.5098
100	1.0898	13.2902	7.5783	0.5301

Table A2.3 Values of vertical strain and void ratio for each load stage for GR-2

Vertical stress Kpa	ΔH	Specimen Height H(mm)	Vertical strain (%)	Void ratio
5.2	-0.6966	15.2166	4.7975	0.6298
25	-0.5740	15.0940	3.9532	0.6167
50	-0.4360	14.9560	3.0028	0.6019
100	-0.1440	14.6640	0.9917	0.5706
200	0.2826	14.2374	-1.9463	0.5249
400	0.7436	13.7764	-5.1212	0.4755
800	1.2440	13.2760	-8.5675	0.4220
400	1.1400	13.3800	-7.8512	0.4331
200	0.9856	13.5344	-6.7879	0.4496
100	0.8040	13.7160	-5.5372	0.4691

Appendix B: Test Reports for Creep Tests

1- Creep Tests for Soft samples GR 1-1

Table B1-1 Creep test for soft sample GR 1-1 OCR=1

Starting date	8/4/2017	
Finishing date	18/4/2017	
Consolidation type =	Fixed ring consolidometer	
Before test		
Mass of the ring(g)	61.77	
Inside diameter of the ring (cm)	4.975	
Height of specimen, H_i (cm)	1.451	
Area of specimen, A (cm ²)	19.44	
Mass of specimen + ring (g)	104.94	
Initial moisture content of specimen, w_i (%)	0.60	
Specific gravity of solids, G_s	2.65	
After test		
Mass of wet sample + ring(g)	100.36	
Mass of can(g)	71.56	
Mass of can + wet soil (g)	85.91	
Mass of wet specimen (g)	38.59	
Mass of can + dry soil (g)	81.45	
Mass of dry specimen, M_d (g)	26.60	
Final moisture content of specimen, w_f %	0.45	
Calculations		
Mass of solids in specimen, M_d (g)		26.5962
Mass of water in specimen before test, M_{wi} (g)	$W_i \times M_d$	15.9577
Mass of water in specimen after test, M_{wf} (g)	$W_f \times M_d$	11.9938
ρ_w		1 g/cm ³
Height of solids, H_s (cm)	$M_d / (A \cdot G_s \cdot \rho_w)$	0.51629
Height of water before test, H_{wi} (cm)	$M_{wi} / (A \cdot \rho_w)$	0.8209
Height of water after test, H_{wf} (cm)	$M_{wf} / (A \cdot \rho_w)$	0.6170
$\Sigma \Delta H$ (cm)		0.216
Height of specimen after test, (cm)		1.2350
Void ratio before test, e_o	$(H_i - H_s) / H_s$	1.8104
Void ratio after test, e_f	$(H_f - H_s) / H_s$	1.3920

Table B1-2 Creep test for soft sample GR 1-1 OCR=1.3

Starting date	8/4/2017	
Finishing date	18/4/2017	
Consolidation type =	Fixed ring consolidometer	
Before test		
Mass of the ring(g)	61.19	
Inside diameter of the ring (cm)	4.97	
Height of specimen, H_i (cm)	1.45	
Area of specimen, A (cm ²)	19.40	
Mass of specimen + ring (g)	108.30	
Initial moisture content of specimen, w_i (%)	0.60	
Specific gravity of solids, G_s	2.65	
After test		
Mass of wet sample + ring(g)	103.06	
Mass of can(g)	65.49	
Mass of can + wet soil (g)	80.15	
Mass of wet specimen (g)	41.87	
Mass of can + dry soil (g)	75.73	
Mass of dry specimen, M_d (g)	29.25	
Final moisture content of specimen, w_f %	0.432	
Calculations		
Mass of solids in specimen, M_d (g)		29.2462
Mass of water in specimen before test, M_{wi} (g)	$W_i \times M_d$	17.5477
Mass of water in specimen after test, M_{wf} (g)	$W_f \times M_d$	12.6238
ρ_w		1 g/cm ³
Height of solids, H_s (cm)	$M_d / (A * G_s * \rho_w)$	0.56888
Height of water before test, H_{wi} (cm)	$M_{wi} / (A * \rho_w)$	0.9045
Height of water after test, H_{wf} (cm)	$M_{wf} / (A * \rho_w)$	0.6507
$\Sigma \Delta H$ (cm)		0.24756
Height of specimen after test, (cm)		1.2044
Void ratio before test, e_o	$(H_i - H_s) / H_s$	1.5524
Void ratio after test, e_f	$(H_f - H_s) / H_s$	1.1172

Table B1-3 Creep test for soft sample GR 1-1 OCR=2

Starting date	8/4/2017	
Finishing date	18/4/2017	
Consolidation type =	Fixed ring consolidometer	
Before test		
Mass of the ring(g)	61.66	
Inside diameter of the ring (cm)	4.972	
Height of specimen, H_i (cm)	1.438	
Area of specimen, A (cm ²)	19.42	
Mass of specimen + ring (g)	102.87	
Initial moisture content of specimen, w_i (%)	0.60	
Specific gravity of solids, G_s	2.65	
After test		
Mass of wet sample + ring(g)	100.71	
Mass of can(g)	71.56	
Mass of can + wet soil (g)	85.21	
Mass of wet specimen (g)	39.05	
Mass of can + dry soil (g)	80.96	
Mass of dry specimen, M_d (g)	26.89	
Final moisture content of specimen, w_f %	0.45	
Calculations		
Mass of solids in specimen, M_d (g)		26.8916
Mass of water in specimen before test, M_{wi} (g)	$W_i \times M_d$	16.1349
Mass of water in specimen after test, M_{wf} (g)	$W_f \times M_d$	12.1584
ρ_w		1 g/cm ³
Height of solids, H_s (cm)	$M_d / (A * G_s * \rho_w)$	0.52266
Height of water before test, H_{wi} (cm)	$M_{wi} / (A * \rho_w)$	0.8310
Height of water after test, H_{wf} (cm)	$M_{wf} / (A * \rho_w)$	0.6262
$\Sigma \Delta H$ (cm)		0.1947
Height of specimen after test, (cm)		1.2433
Void ratio before test, e_o	$(H_i - H_s) / H_s$	1.7513
Void ratio after test, e_f	$(H_f - H_s) / H_s$	1.3788

Table B1-4 Creep test for soft sample GR 1-1 OCR=4

Starting date	8/4/2017	
Finishing date	18/4/2017	
Consolidation type =	Fixed ring consolidometer	
Before test		
Mass of the ring(g)	61.19	
Inside diameter of the ring (cm)	4.970	
Height of specimen, H_i (cm)	1.452	
Area of specimen, A (cm ²)	19.40	
Mass of specimen + ring (g)	107.67	
Initial moisture content of specimen, w_i (%)	0.60	
Specific gravity of solids, G_s	2.65	
After test		
Mass of wet sample + ring(g)	103.52	
Mass of can(g)	47.61	
Mass of can + wet soil (g)	64.05	
Mass of wet specimen (g)	42.33	
Mass of can + dry soil (g)	58.85	
Mass of dry specimen, M_d (g)	28.94	
Final moisture content of specimen, w_f %	0.46	
Calculations		
Mass of solids in specimen, M_d (g)		28.9409
Mass of water in specimen before test, M_{wi} (g)	$W_i \times M_d$	17.3646
Mass of water in specimen after test, M_{wf} (g)	$W_f \times M_d$	13.3891
ρ_w		1 g/cm ³
Height of solids, H_s (cm)	$M_d / (A * G_s * \rho_w)$	0.56294
Height of water before test, H_{wi} (cm)	$M_{wi} / (A * \rho_w)$	0.8951
Height of water after test, H_{wf} (cm)	$M_{wf} / (A * \rho_w)$	0.6902
$\Sigma \Delta H$ (cm)		0.18614
Height of specimen after test, (cm)		1.2659
Void ratio before test, e_o	$(H_i - H_s) / H_s$	1.5793
Void ratio after test, e_f	$(H_f - H_s) / H_s$	1.2486

2- Creep Tests for Soft samples GR 1-2

Table B2-1 Creep test for soft sample GR 1-2 OCR=1

Starting date	8/4/2017	
Finishing date	18/4/2017	
Consolidation type =	Fixed ring consolidometer	
Before test		
Mass of the ring(g)	61.44	
Inside diameter of the ring (cm)	4.98	
Height of specimen, H_i (cm)	1.44	
Area of specimen, A (cm ²)	19.48	
Mass of specimen + ring (g)	102.36	
Initial moisture content of specimen, w_i (%)	0.60	
Specific gravity of solids, G_s	2.65	
After test		
Mass of wet sample + ring(g)	92.26	
Mass of can(g)	47.62	
Mass of can + wet soil (g)	65.66	
Mass of wet specimen (g)	30.82	
Mass of can + dry soil (g)	60.36	
Mass of dry specimen, M_d (g)	21.77	
Final moisture content of specimen, w_f %	0.416	
Calculations		
Mass of solids in specimen, M_d (g)		21.7653
Mass of water in specimen before test, M_{wi} (g)	$W_i \times M_d$	13.0592
Mass of water in specimen after test, M_{wf} (g)	$W_f \times M_d$	9.0547
ρ_w		1 g/cm ³
Height of solids, H_s (cm)	$M_d / (A * G_s * \rho_w)$	0.42167
Height of water before test, H_{wi} (cm)	$M_{wi} / (A * \rho_w)$	0.6705
Height of water after test, H_{wf} (cm)	$M_{wf} / (A * \rho_w)$	0.4649
$\Sigma \Delta H$ (cm)		0.2969
Height of specimen after test, (cm)		1.1381
Void ratio before test, e_o	$(H_i - H_s) / H_s$	2.4031
Void ratio after test, e_f	$(H_f - H_s) / H_s$	1.6990

Table B2-2 Creep test for soft sample GR 1-2 OCR=1.3

Starting date	8/4/2017	
Finishing date	18/4/2017	
Consolidation type =	Fixed ring consolidometer	
Before test		
Mass of the ring(g)	36.20	
Inside diameter of the ring (cm)	4.98	
Height of specimen, H_i (cm)	1.41	
Area of specimen, A (cm ²)	19.45	
Mass of specimen + ring (g)	77.48	
Initial moisture content of specimen, w_i (%)	0.60	
Specific gravity of solids, G_s	2.65	
After test		
Mass of wet sample + ring(g)	72.51	
Mass of can(g)	71.56	
Mass of can + wet soil (g)	88.13	
Mass of wet specimen (g)	36.31	
Mass of can + dry soil (g)	83.21	
Mass of dry specimen, M_d (g)	25.53	
Final moisture content of specimen, w_f %	0.42	
Calculations		
Mass of solids in specimen, M_d (g)		25.5288
Mass of water in specimen before test, M_{wi} (g)	$W_i \times M_d$	15.3173
Mass of water in specimen after test, M_{wf} (g)	$W_f \times M_d$	10.7812
ρ_w		1 g/cm ³
Height of solids, H_s (cm)	$M_d / (A * G_s * \rho_w)$	0.49537
Height of water before test, H_{wi} (cm)	$M_{wi} / (A * \rho_w)$	0.7876
Height of water after test, H_{wf} (cm)	$M_{wf} / (A * \rho_w)$	0.5544
$\Sigma \Delta H$ (cm)		0.2625
Height of specimen after test, (cm)		1.1495
Void ratio before test, e_o	$(H_i - H_s) / H_s$	1.8504
Void ratio after test, e_f	$(H_f - H_s) / H_s$	1.3205

Table B2-3 Creep test for soft sample GR 1-2 OCR=2

Starting date	8/4/2017	
Finishing date	18/4/2017	
Consolidation type =	Fixed ring consolidometer	
Before test		
Mass of the ring(g)	60.60	
Inside diameter of the ring (cm)	4.98	
Height of specimen, H_i (cm)	1.43	
Area of specimen, A (cm ²)	19.49	
Mass of specimen + ring (g)	106.00	
Initial moisture content of specimen, w_i (%)	0.60	
Specific gravity of solids, G_s	2.65	
After test		
Mass of wet sample + ring(g)	98.25	
Mass of can(g)	47.62	
Mass of can + wet soil (g)	61.43	
Mass of wet specimen (g)	37.65	
Mass of can + dry soil (g)	57.25	
Mass of dry specimen, M_d (g)	26.25	
Final moisture content of specimen, w_f %	0.434	
Calculations		
Mass of solids in specimen, M_d (g)		26.2541
Mass of water in specimen before test, M_{wi} (g)	$W_i \times M_d$	15.7525
Mass of water in specimen after test, M_{wf} (g)	$W_f \times M_d$	11.3959
ρ_w		1 g/cm ³
Height of solids, H_s (cm)	$M_d / (A \times G_s \times \rho_w)$	0.50822
Height of water before test, H_{wi} (cm)	$M_{wi} / (A \times \rho_w)$	0.8081
Height of water after test, H_{wf} (cm)	$M_{wf} / (A \times \rho_w)$	0.5846
$\Sigma \Delta H$ (cm)		0.25982
Height of specimen after test, (cm)		1.1712
Void ratio before test, e_o	$(H_i - H_s) / H_s$	1.8157
Void ratio after test, e_f	$(H_f - H_s) / H_s$	1.3045

Table B2-4 Creep test for soft sample GR 1-2 OCR=4

Starting date	8/4/2017	
Finishing date	18/4/2017	
Consolidation type =	Fixed ring consolidometer	
Before test		
Mass of the ring(g)	61.81	
Inside diameter of the ring (cm)	4.98	
Height of specimen, Hi (cm)	1.43	
Area of specimen, A (cm ²)	19.48	
Mass of specimen + ring (g)	103.04	
Initial moisture content of specimen, wi (%)	0.60	
Specific gravity of solids, Gs	2.65	
After test		
Mass of wet sample + ring(g)	101.10	
Mass of can(g)	47.60	
Mass of can + wet soil (g)	62.00	
Mass of wet specimen (g)	39.29	
Mass of can + dry soil (g)	57.70	
Mass of dry specimen, Md (g)	27.56	
Final moisture content of specimen, wf %	0.426	
Calculations		
Mass of solids in specimen, Md (g)		27.5576
Mass of water in specimen before test, Mwi (g)	$W_i \times M_d$	16.5345
Mass of water in specimen after test, Mwf (g)	$W_f \times M_d$	11.7324
ρ_w		1 g/cm ³
Height of solids, Hs (cm)	$M_d / (A * G_s * \rho_w)$	0.53388
Height of water before test, Hwi (cm)	$M_{wi} / (A * \rho_w)$	0.8489
Height of water after test, Hwf (cm)	$M_{wf} / (A * \rho_w)$	0.6023
$\Sigma \Delta H$ (cm)		0.18614
Height of specimen after test, (cm)		1.2115
Void ratio before test, e _o	$(H_i - H_s) / H_s$	1.6841
Void ratio after test, e _f	$(H_f - H_s) / H_s$	1.2692

3- Creep Tests for Soft samples GR 1-3

Table B3-1 Creep test for soft sample GR 1-3 OCR=1

Starting date	25/6/2017	
Finishing date	6/7/2017	
Consolidation type =	Fixed ring consolidometer	
Before test		
Mass of the ring(g)	60.76	
Inside diameter of the ring (cm)	4.975	
Height of specimen, H_i (cm)	1.451	
Area of specimen, A (cm ²)	19.44	
Mass of specimen + ring (g)	105.60	
Initial moisture content of specimen, w_i (%)	59.00	
Specific gravity of solids, G_s	2.65	
After test		
Mass of wet sample + ring(g)	99.03	
Mass of can(g)	76.11	
Mass of can + wet soil (g)	86.96	
Mass of wet specimen (g)	38.27	
Mass of can + dry soil (g)	84.04	
Mass of dry specimen, M_d (g)	27.97	
Final moisture content of specimen, w_f %	0.37	
Calculations		
Mass of solids in specimen, M_d (g)		27.9706
Mass of water in specimen before test, M_{wi} (g)	$W_i \times M_d$	1650.2659
Mass of water in specimen after test, M_{wf} (g)	$W_f \times M_d$	10.2994
ρ_w		1 g/cm ³
Height of solids, H_s (cm)	$M_d / (A * G_s * \rho_w)$	0.54298
Height of water before test, H_{wi} (cm)	$M_{wi} / (A * \rho_w)$	84.8942
Height of water after test, H_{wf} (cm)	$M_{wf} / (A * \rho_w)$	0.5298
$\Sigma \Delta H$ (cm)		0.3356
Height of specimen after test, (cm)		1.1154
Void ratio before test, e_o	$(H_i - H_s) / H_s$	1.6723
Void ratio after test, e_f	$(H_f - H_s) / H_s$	1.0542

Table B3-2 Creep test for soft sample GR 1-3 OCR=1.3

Starting date	25/6/2017	
Finishing date	6/7/2017	
Consolidation type =	Fixed ring consolidometer	
Before test		
Mass of the ring(g)	61.66	
Inside diameter of the ring (cm)	4.972	
Height of specimen, H_i (cm)	1.438	
Area of specimen, A (cm ²)	19.42	
Mass of specimen + ring (g)	107.18	
Initial moisture content of specimen, w_i (%)	0.59	
Specific gravity of solids, G_s	2.65	
After test		
Mass of wet sample + ring(g)	100.68	
Mass of can(g)	49.80	
Mass of can + wet soil (g)	62.13	
Mass of wet specimen (g)	39.02	
Mass of can + dry soil (g)	58.76	
Mass of dry specimen, M_d (g)	28.36	
Final moisture content of specimen, w_f %	0.38	
Calculations		
Mass of solids in specimen, M_d (g)		28.3552
Mass of water in specimen before test, M_{wi} (g)	$W_i \times M_d$	16.7295
Mass of water in specimen after test, M_{wf} (g)	$W_f \times M_d$	10.6648
ρ_w		1 g/cm ³
Height of solids, H_s (cm)	$M_d / (A * G_s * \rho_w)$	0.55110
Height of water before test, H_{wi} (cm)	$M_{wi} / (A * \rho_w)$	0.8617
Height of water after test, H_{wf} (cm)	$M_{wf} / (A * \rho_w)$	0.5493
$\Sigma \Delta H$ (cm)		0.3406
Height of specimen after test, (cm)		1.0974
Void ratio before test, e_o	$(H_i - H_s) / H_s$	1.6093
Void ratio after test, e_f	$(H_f - H_s) / H_s$	0.9913

Table B3-3 Creep test for soft sample GR 1-3 OCR=2

Starting date	25/6/2017	
Finishing date	6/7/2017	
Consolidation type =	Fixed ring consolidometer	
Before test		
Mass of the ring(g)	60.27	
Inside diameter of the ring (cm)	4.986	
Height of specimen, H_i (cm)	1.445	
Area of specimen, A (cm ²)	19.53	
Mass of specimen + ring (g)	106.11	
Initial moisture content of specimen, w_i (%)	0.59	
Specific gravity of solids, G_s	2.65	
After test		
Mass of wet sample + ring(g)	99.78	
Mass of can(g)	76.11	
Mass of can + wet soil (g)	92.05	
Mass of wet specimen (g)	39.51	
Mass of can + dry soil (g)	87.65	
Mass of dry specimen, M_d (g)	28.60	
Final moisture content of specimen, w_f %	0.38	
Calculations		
Mass of solids in specimen, M_d (g)		28.6039
Mass of water in specimen before test, M_{wi} (g)	$W_i \times M_d$	16.8763
Mass of water in specimen after test, M_{wf} (g)	$W_f \times M_d$	10.9061
ρ_w		1 g/cm ³
Height of solids, H_s (cm)	$M_d / (A * G_s * \rho_w)$	0.55282
Height of water before test, H_{wi} (cm)	$M_{wi} / (A * \rho_w)$	0.8643
Height of water after test, H_{wf} (cm)	$M_{wf} / (A * \rho_w)$	0.5586
$\Sigma \Delta H$ (cm)		0.3262
Height of specimen after test, (cm)		1.1188
Void ratio before test, e_o	$(H_i - H_s) / H_s$	1.6139
Void ratio after test, e_f	$(H_f - H_s) / H_s$	1.0238

Table B3-4 Creep test for soft sample GR 1-3 OCR=4

Starting date	25/6/2017	
Finishing date	6/7/2017	
Consolidation type =	Fixed ring consolidometer	
Before test		
Mass of the ring(g)	61.19	
Inside diameter of the ring (cm)	4.97	
Height of specimen, H_i (cm)	1.45	
Area of specimen, A (cm ²)	19.40	
Mass of specimen + ring (g)	107.01	
Initial moisture content of specimen, w_i (%)	59.00	
Specific gravity of solids, G_s	2.65	
After test		
Mass of wet sample + ring(g)	101.07	
Mass of can(g)	49.81	
Mass of can + wet soil (g)	61.18	
Mass of wet specimen (g)	39.88	
Mass of can + dry soil (g)	57.97	
Mass of dry specimen, M_d (g)	28.62	
Final moisture content of specimen, w_f %	0.393	
Calculations		
Mass of solids in specimen, M_d (g)		28.6210
Mass of water in specimen before test, M_{wi} (g)	$W_i \times M_d$	1688.6392
Mass of water in specimen after test, M_{wf} (g)	$W_f \times M_d$	11.2590
ρ_w		1 g/cm ³
Height of solids, H_s (cm)	$M_d / (A * G_s * \rho_w)$	0.55672
Height of water before test, H_{wi} (cm)	$M_{wi} / (A * \rho_w)$	87.0431
Height of water after test, H_{wf} (cm)	$M_{wf} / (A * \rho_w)$	0.5804
$\Sigma \Delta H$ (cm)		0.3029
Height of specimen after test, (cm)		1.1491
Void ratio before test, e_o	$(H_i - H_s) / H_s$	1.6081
Void ratio after test, e_f	$(H_f - H_s) / H_s$	1.0641

4- Creep Tests for Soft samples GR 1-4

Table B4-1 Creep test for soft sample GR 1-4 OCR=1

Starting date	19/5/2017	
Finishing date	30/5/2017	
Consolidation type =	Fixed ring consolidometer	
Before test		
Mass of the ring(g)	61.66	
Inside diameter of the ring (cm)	4.972	
Height of specimen, H_i (cm)	1.438	
Area of specimen, A (cm ²)	19.42	
Mass of specimen + ring (g)	109.33	
Initial moisture content of specimen, w_i (%)	0.61	
Specific gravity of solids, G_s	2.65	
After test		
Mass of wet sample + ring(g)	101.48	
Mass of can(g)	47.62	
Mass of can + wet soil (g)	68.85	
Mass of wet specimen (g)	39.82	
Mass of can + dry soil (g)	63.25	
Mass of dry specimen, M_d (g)	29.32	
Final moisture content of specimen, w_f %	0.36	
Calculations		
Mass of solids in specimen, M_d (g)		29.3164
Mass of water in specimen before test, M_{wi} (g)	$W_i \times M_d$	17.9416
Mass of water in specimen after test, M_{wf} (g)	$W_f \times M_d$	10.5036
ρ_w		1 g/cm ³
Height of solids, H_s (cm)	$M_d / (A * G_s * \rho_w)$	0.56979
Height of water before test, H_{wi} (cm)	$M_{wi} / (A * \rho_w)$	0.9241
Height of water after test, H_{wf} (cm)	$M_{wf} / (A * \rho_w)$	0.5410
$\Sigma \Delta H$ (cm)		0.463
Height of specimen after test, (cm)		0.9750
Void ratio before test, e_o	$(H_i - H_s) / H_s$	1.5238
Void ratio after test, e_f	$(H_f - H_s) / H_s$	0.7112

Table B4-2 Creep test for soft sample GR 1-4 OCR=1.3

Starting date	19/5/2017	
Finishing date	30/5/2017	
Consolidation type =	Fixed ring consolidometer	
Before test		
Mass of the ring(g)	60.27	
Inside diameter of the ring (cm)	4.986	
Height of specimen, H_i (cm)	1.445	
Area of specimen, A (cm ²)	19.53	
Mass of specimen + ring (g)	104.65	
Initial moisture content of specimen, w_i (%)	0.61	
Specific gravity of solids, G_s	2.65	
After test		
Mass of wet sample + ring(g)	97.55	
Mass of can(g)	82.69	
Mass of can + wet soil (g)	107.61	
Mass of wet specimen (g)	37.28	
Mass of can + dry soil (g)	100.91	
Mass of dry specimen, M_d (g)	27.26	
Final moisture content of specimen, w_f %	0.37	
Calculations		
Mass of solids in specimen, M_d (g)		27.2569
Mass of water in specimen before test, M_{wi} (g)	$W_i \times M_d$	16.6812
Mass of water in specimen after test, M_{wf} (g)	$W_f \times M_d$	10.0231
ρ_w		1 g/cm ³
Height of solids, H_s (cm)	$M_d / (A * G_s * \rho_w)$	0.52679
Height of water before test, H_{wi} (cm)	$M_{wi} / (A * \rho_w)$	0.8543
Height of water after test, H_{wf} (cm)	$M_{wf} / (A * \rho_w)$	0.5133
$\Sigma \Delta H$ (cm)		0.3994
Height of specimen after test, (cm)		1.0456
Void ratio before test, e_o	$(H_i - H_s) / H_s$	1.7430
Void ratio after test, e_f	$(H_f - H_s) / H_s$	0.9849

Table B4-3 Creep test for soft sample GR 1-4 OCR=2

Starting date	19/5/2017	
Finishing date	30/5/2017	
Consolidation type =	Fixed ring consolidometer	
Before test		
Mass of the ring(g)	61.19	
Inside diameter of the ring (cm)	4.97	
Height of specimen, H_i (cm)	1.45	
Area of specimen, A (cm ²)	19.40	
Mass of specimen + ring (g)	108.13	
Initial moisture content of specimen, w_i (%)	0.61	
Specific gravity of solids, G_s	2.65	
After test		
Mass of wet sample + ring(g)	100.86	
Mass of can(g)	69.40	
Mass of can + wet soil (g)	80.22	
Mass of wet specimen (g)	39.67	
Mass of can + dry soil (g)	77.26	
Mass of dry specimen, M_d (g)	28.82	
Final moisture content of specimen, w_f %	0.377	
Calculations		
Mass of solids in specimen, M_d (g)		28.8176
Mass of water in specimen before test, M_{wi} (g)	$W_i \times M_d$	17.6364
Mass of water in specimen after test, M_{wf} (g)	$W_f \times M_d$	10.8524
ρ_w		1 g/cm ³
Height of solids, H_s (cm)	$M_d / (A * G_s * \rho_w)$	0.56054
Height of water before test, H_{wi} (cm)	$M_{wi} / (A * \rho_w)$	0.9091
Height of water after test, H_{wf} (cm)	$M_{wf} / (A * \rho_w)$	0.5594
$\Sigma \Delta H$ (cm)		0.4004
Height of specimen after test, (cm)		1.0516
Void ratio before test, e_o	$(H_i - H_s) / H_s$	1.5903
Void ratio after test, e_f	$(H_f - H_s) / H_s$	0.8760

Table B4-4 Creep test for soft sample GR 1-4 OCR=4

Starting date	19/5/2017	
Finishing date	30/5/2017	
Consolidation type =	Fixed ring consolidometer	
Before test		
Mass of the ring(g)	61.66	
Inside diameter of the ring (cm)	4.972	
Height of specimen, H_i (cm)	1.438	
Area of specimen, A (cm ²)	19.42	
Mass of specimen + ring (g)	107.58	
Initial moisture content of specimen, w_i (%)	0.61	
Specific gravity of solids, G_s	2.65	
After test		
Mass of wet sample + ring(g)	100.05	
Mass of can(g)	71.55	
Mass of can + wet soil (g)	90.75	
Mass of wet specimen (g)	38.39	
Mass of can + dry soil (g)	85.72	
Mass of dry specimen, M_d (g)	28.33	
Final moisture content of specimen, w_f %	0.35	
Calculations		
Mass of solids in specimen, M_d (g)		28.3326
Mass of water in specimen before test, M_{wi} (g)	$W_i \times M_d$	17.3396
Mass of water in specimen after test, M_{wf} (g)	$W_f \times M_d$	10.0574
ρ_w		1 g/cm ³
Height of solids, H_s (cm)	$M_d / (A * G_s * \rho_w)$	0.55067
Height of water before test, H_{wi} (cm)	$M_{wi} / (A * \rho_w)$	0.8931
Height of water after test, H_{wf} (cm)	$M_{wf} / (A * \rho_w)$	0.5180
$\Sigma \Delta H$ (cm)		0.38324
Height of specimen after test, (cm)		1.0548
Void ratio before test, e_o	$(H_i - H_s) / H_s$	1.6114
Void ratio after test, e_f	$(H_f - H_s) / H_s$	0.9154

5- Creep Tests for Compacted samples GR 2

Table B5-1 Creep test for compacted sample GR-2 OCR=1

Starting date	13/6/2017	
Finishing date	23/6/2017	
Consolidation type =	Fixed ring consolidometer	
Before test		
Mass of the ring(g)	60.76	
Inside diameter of the ring (cm)	4.975	
Height of specimen, H_i (cm)	1.451	
Area of specimen, A (cm ²)	19.44	
Mass of specimen + ring (g)	116.24	
Initial moisture content of specimen, w_i (%)	0.28	
Specific gravity of solids, G_s	2.65	
After test		
Mass of wet sample + ring(g)	117.59	
Mass of can(g)	49.80	
Mass of can + wet soil (g)	59.00	
Mass of wet specimen (g)	56.83	
Mass of can + dry soil (g)	56.84	
Mass of dry specimen, M_d (g)	43.49	
Final moisture content of specimen, w_f %	0.31	
Calculations		
Mass of solids in specimen, M_d (g)		43.4873
Mass of water in specimen before test, M_{wi} (g)	$W_i \times M_d$	12.1764
Mass of water in specimen after test, M_{wf} (g)	$W_f \times M_d$	13.3427
ρ_w		1 g/cm ³
Height of solids, H_s (cm)	$M_d / (A \cdot G_s \cdot \rho_w)$	0.84419
Height of water before test, H_{wi} (cm)	$M_{wi} / (A \cdot \rho_w)$	0.6264
Height of water after test, H_{wf} (cm)	$M_{wf} / (A \cdot \rho_w)$	0.6864
$\Sigma \Delta H$ (cm)		0.0045
Height of specimen after test, (cm)		1.4465
Void ratio before test, e_o	$(H_i - H_s) / H_s$	0.7188
Void ratio after test, e_f	$(H_f - H_s) / H_s$	0.7135

Table B5-2 Creep test for compacted sample GR-2 OCR=1.3

Starting date	13/6/2017	
Finishing date	23/6/2017	
Consolidation type =	Fixed ring consolidometer	
Before test		
Mass of the ring(g)	61.66	
Inside diameter of the ring (cm)	4.972	
Height of specimen, H_i (cm)	1.438	
Area of specimen, A (cm ²)	19.42	
Mass of specimen + ring (g)	118.56	
Initial moisture content of specimen, w_i (%)	0.28	
Specific gravity of solids, G_s	2.65	
After test		
Mass of wet sample + ring(g)	119.67	
Mass of can(g)	82.69	
Mass of can + wet soil (g)	96.40	
Mass of wet specimen (g)	58.01	
Mass of can + dry soil (g)	93.18	
Mass of dry specimen, M_d (g)	44.39	
Final moisture content of specimen, w_f %	0.31	
Calculations		
Mass of solids in specimen, M_d (g)		44.3855
Mass of water in specimen before test, M_{wi} (g)	$W_i \times M_d$	12.4279
Mass of water in specimen after test, M_{wf} (g)	$W_f \times M_d$	13.6245
ρ_w		1 g/cm ³
Height of solids, H_s (cm)	$M_d / (A * G_s * \rho_w)$	0.86267
Height of water before test, H_{wi} (cm)	$M_{wi} / (A * \rho_w)$	0.6401
Height of water after test, H_{wf} (cm)	$M_{wf} / (A * \rho_w)$	0.7017
$\Sigma \Delta H$ (cm)		-0.0031
Height of specimen after test, (cm)		1.4411
Void ratio before test, e_o	$(H_i - H_s) / H_s$	0.6669
Void ratio after test, e_f	$(H_f - H_s) / H_s$	0.6705

Table B5-3 Creep test for compacted sample GR-2 OCR=2

Starting date	13/6/2017	
Finishing date	23/6/2017	
Consolidation type =	Fixed ring consolidometer	
Before test		
Mass of the ring(g)	60.27	
Inside diameter of the ring (cm)	4.986	
Height of specimen, H_i (cm)	1.445	
Area of specimen, A (cm ²)	19.53	
Mass of specimen + ring (g)	117.13	
Initial moisture content of specimen, w_i (%)	0.28	
Specific gravity of solids, G_s	2.65	
After test		
Mass of wet sample + ring(g)	118.55	
Mass of can(g)	49.81	
Mass of can + wet soil (g)	61.69	
Mass of wet specimen (g)	58.28	
Mass of can + dry soil (g)	58.86	
Mass of dry specimen, M_d (g)	44.40	
Final moisture content of specimen, w_f %	0.31	
Calculations		
Mass of solids in specimen, M_d (g)		44.3968
Mass of water in specimen before test, M_{wi} (g)	$W_i \times M_d$	12.4311
Mass of water in specimen after test, M_{wf} (g)	$W_f \times M_d$	13.8832
ρ_w		1 g/cm ³
Height of solids, H_s (cm)	$M_d / (A * G_s * \rho_w)$	0.85805
Height of water before test, H_{wi} (cm)	$M_{wi} / (A * \rho_w)$	0.6367
Height of water after test, H_{wf} (cm)	$M_{wf} / (A * \rho_w)$	0.7110
$\Sigma \Delta H$ (cm)		0.0006
Height of specimen after test, (cm)		1.4444
Void ratio before test, e_o	$(H_i - H_s) / H_s$	0.6841
Void ratio after test, e_f	$(H_f - H_s) / H_s$	0.6834

Table B5-4 Creep test for compacted sample GR-2 OCR=4

Starting date	13/6/2017	
Finishing date	23/6/2017	
Consolidation type =	Fixed ring consolidometer	
Before test		
Mass of the ring(g)	61.19	
Inside diameter of the ring (cm)	4.97	
Height of specimen, Hi (cm)	1.45	
Area of specimen, A (cm ²)	19.40	
Mass of specimen + ring (g)	117.70	
Initial moisture content of specimen, wi (%)	0.28	
Specific gravity of solids, Gs	2.65	
After test		
Mass of wet sample + ring(g)	119.76	
Mass of can(g)	49.81	
Mass of can + wet soil (g)	64.08	
Mass of wet specimen (g)	58.57	
Mass of can + dry soil (g)	60.65	
Mass of dry specimen, Md (g)	44.49	
Final moisture content of specimen, wf %	0.316	
Calculations		
Mass of solids in specimen, Md (g)		44.4919
Mass of water in specimen before test, Mwi (g)	$W_i \times M_d$	12.4577
Mass of water in specimen after test, Mwf (g)	$W_f \times M_d$	14.0781
ρ_w		1 g/cm ³
Height of solids, Hs (cm)	$M_d / (A * G_s * \rho_w)$	0.86543
Height of water before test, Hwi (cm)	$M_{wi} / (A * \rho_w)$	0.6421
Height of water after test, Hwf (cm)	$M_{wf} / (A * \rho_w)$	0.7257
$\Sigma \Delta H$ (cm)		-0.0537
Height of specimen after test, (cm)		1.5057
Void ratio before test, e _o	$(H_i - H_s) / H_s$	0.6778
Void ratio after test, e _f	$(H_f - H_s) / H_s$	0.7398

6- Creep Tests for Compacted samples GR 3

Table B6-1 Creep test for compacted sample GR-3 OCR=1

Starting date	17/7/2017	
Finishing date	28/7/2017	
Consolidation type =	Fixed ring consolidometer	
Before test		
Mass of the ring(g)	60.76	
Inside diameter of the ring (cm)	4.975	
Height of specimen, H_i (cm)	1.451	
Area of specimen, A (cm ²)	19.44	
Mass of specimen + ring (g)	119.81	
Initial moisture content of specimen, w_i (%)	0.23	
Specific gravity of solids, G_s	2.65	
After test		
Mass of wet sample + ring(g)	121.97	
Mass of can(g)	82.69	
Mass of can + wet soil (g)	104.21	
Mass of wet specimen (g)	61.21	
Mass of can + dry soil (g)	99.13	
Mass of dry specimen, M_d (g)	46.76	
Final moisture content of specimen, w_f %	0.31	
Calculations		
Mass of solids in specimen, M_d (g)		46.7608
Mass of water in specimen before test, M_{wi} (g)	$W_i \times M_d$	10.7550
Mass of water in specimen after test, M_{wf} (g)	$W_f \times M_d$	14.4492
ρ_w		1 g/cm ³
Height of solids, H_s (cm)	$M_d / (A * G_s * \rho_w)$	0.90774
Height of water before test, H_{wi} (cm)	$M_{wi} / (A * \rho_w)$	0.5533
Height of water after test, H_{wf} (cm)	$M_{wf} / (A * \rho_w)$	0.7433
$\Sigma \Delta H$ (cm)		-0.0346
Height of specimen after test, (cm)		1.4856
Void ratio before test, e_o	$(H_i - H_s) / H_s$	0.5985
Void ratio after test, e_f	$(H_f - H_s) / H_s$	0.6366

Table B6-2 Creep test for compacted sample GR-3 OCR=1.3

Starting date	17/7/2017	
Finishing date	28/7/2017	
Consolidation type =	Fixed ring consolidometer	
Before test		
Mass of the ring(g)	61.66	
Inside diameter of the ring (cm)	4.972	
Height of specimen, Hi (cm)	1.438	
Area of specimen, A (cm ²)	19.42	
Mass of specimen + ring (g)	120.47	
Initial moisture content of specimen, wi (%)	0.23	
Specific gravity of solids, Gs	2.65	
After test		
Mass of wet sample + ring(g)	122.98	
Mass of can(g)	65.49	
Mass of can + wet soil (g)	77.79	
Mass of wet specimen (g)	61.32	
Mass of can + dry soil (g)	74.89	
Mass of dry specimen, Md (g)	46.86	
Final moisture content of specimen, wf %	0.31	
Calculations		
Mass of solids in specimen, Md (g)		46.8624
Mass of water in specimen before test, Mwi (g)	$W_i \times M_d$	10.7784
Mass of water in specimen after test, Mwf (g)	$W_f \times M_d$	14.4576
ρ_w		1 g/cm ³
Height of solids, Hs (cm)	$M_d / (A \times G_s \times \rho_w)$	0.91081
Height of water before test, Hwi (cm)	$M_{wi} / (A \times \rho_w)$	0.5551
Height of water after test, Hwf (cm)	$M_{wf} / (A \times \rho_w)$	0.7446
$\Sigma \Delta H$ (cm)		-0.043
Height of specimen after test, (cm)		1.4810
Void ratio before test, e _o	$(H_i - H_s) / H_s$	0.5788
Void ratio after test, e _f	$(H_f - H_s) / H_s$	0.6260

Table B6-3 Creep test for compacted sample GR-2 OCR=2

Starting date	17/7/2017	
Finishing date	28/7/2017	
Consolidation type =	Fixed ring consolidometer	
Before test		
Mass of the ring(g)	60.27	
Inside diameter of the ring (cm)	4.986	
Height of specimen, H_i (cm)	1.445	
Area of specimen, A (cm ²)	19.53	
Mass of specimen + ring (g)	119.12	
Initial moisture content of specimen, w_i (%)	0.23	
Specific gravity of solids, G_s	2.65	
After test		
Mass of wet sample + ring(g)	121.65	
Mass of can(g)	71.55	
Mass of can + wet soil (g)	85.17	
Mass of wet specimen (g)	61.38	
Mass of can + dry soil (g)	81.95	
Mass of dry specimen, M_d (g)	46.87	
Final moisture content of specimen, w_f %	0.31	
Calculations		
Mass of solids in specimen, M_d (g)		46.8687
Mass of water in specimen before test, M_{wi} (g)	$W_i \times M_d$	10.7798
Mass of water in specimen after test, M_{wf} (g)	$W_f \times M_d$	14.5113
ρ_w		1 g/cm ³
Height of solids, H_s (cm)	$M_d / (A * G_s * \rho_w)$	0.90582
Height of water before test, H_{wi} (cm)	$M_{wi} / (A * \rho_w)$	0.5521
Height of water after test, H_{wf} (cm)	$M_{wf} / (A * \rho_w)$	0.7432
$\Sigma \Delta H$ (cm)		-0.0385
Height of specimen after test, (cm)		1.4835
Void ratio before test, e_o	$(H_i - H_s) / H_s$	0.5952
Void ratio after test, e_f	$(H_f - H_s) / H_s$	0.6377

Table B6-4 Creep test for compacted sample GR-2 OCR=4

Starting date	17/7/2017	
Finishing date	28/7/2017	
Consolidation type =	Fixed ring consolidometer	
Before test		
Mass of the ring(g)	60.19	
Inside diameter of the ring (cm)	4.97	
Height of specimen, H_i (cm)	1.45	
Area of specimen, A (cm ²)	19.40	
Mass of specimen + ring (g)	119.76	
Initial moisture content of specimen, w_i (%)	0.23	
Specific gravity of solids, G_s	2.65	
After test		
Mass of wet sample + ring(g)	121.89	
Mass of can(g)	49.81	
Mass of can + wet soil (g)	66.42	
Mass of wet specimen (g)	61.70	
Mass of can + dry soil (g)	62.44	
Mass of dry specimen, M_d (g)	46.92	
Final moisture content of specimen, w_f %	0.315	
Calculations		
Mass of solids in specimen, M_d (g)		46.9158
Mass of water in specimen before test, M_{wi} (g)	$W_i \times M_d$	10.7906
Mass of water in specimen after test, M_{wf} (g)	$W_f \times M_d$	14.7842
ρ_w		1 g/cm ³
Height of solids, H_s (cm)	$M_d / (A * G_s * \rho_w)$	0.91258
Height of water before test, H_{wi} (cm)	$M_{wi} / (A * \rho_w)$	0.5562
Height of water after test, H_{wf} (cm)	$M_{wf} / (A * \rho_w)$	0.7621
$\Sigma \Delta H$ (cm)		-0.04566
Height of specimen after test, (cm)		1.4977
Void ratio before test, e_o	$(H_i - H_s) / H_s$	0.5911
Void ratio after test, e_f	$(H_f - H_s) / H_s$	0.6411